JCI The Journal of Clinical Investigation

SUCNR1 regulates insulin secretion and glucose elevates the succinate response in people with prediabetes

Joan Sabadell-Basallote, … , Joan Vendrell, Sonia Fernández-Veledo

J Clin Invest. 2024. https://doi.org/10.1172/JCI173214.

Research In-Press Preview **Endocrinology** **Metabolism**

Graphical abstract

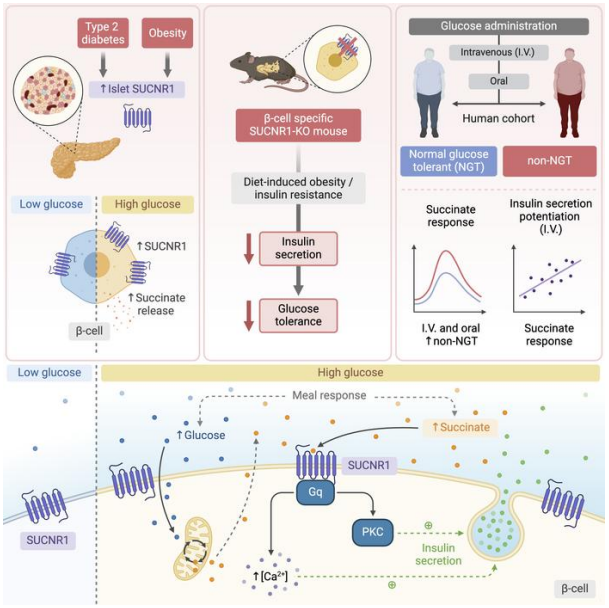

Find the latest version:

https://jci.me/173214/pdf

SUCNR1 Regulates Insulin Secretion and Glucose Elevates the Succinate Response in People with Prediabetes

Joan Sabadell-Basallote[1-4], Brenno Astiarraga[1,2], Carlos Castaño[1,2], Miriam Ejarque[1,2], Maria Repollés-de-Dalmau[1-3], Ivan Quesada[2,5], Jordi Blanco[3], Catalina Núñez-Roa[1,2], M-Mar Rodríguez-Peña[1,2], Laia Martínez[1], Dario F. De Jesus[4], Laura Marroquí[2,5], Ramon Bosch[1,3,6], Eduard Montanya[2,7], Francesc Sureda[3], Andrea Tura[8], Andrea Mari[8], Rohit N. Kulkarni[4], Joan Vendrell[1-3,9], Sonia Fernández-Veledo[1-3,9]

[1] Unitat de Recerca, Hospital Universitari Joan XXIII, Institut d'Investigació Sanitària Pere Virgili, Tarragona, 43005, Spain.

[2] CIBER de Diabetes y Enfermedades Metabólicas Asociadas (CIBERDEM), Instituto de Salud Carlos III, Madrid, 28029, Spain.

[3] Universitat Rovira i Virgili, Tarragona, 43003, Spain.

[4] Islet Cell and Regenerative Biology, Joslin Diabetes Center, Department of Medicine, Beth Israel Deaconess Medical Center, Harvard Stem Cell Institute, Harvard Medical School, Boston, MA, 02215, USA.

[5] Instituto de Investigación, Desarrollo e Innovación en Biotecnología Sanitaria de Elche (IDiBE), Universidad Miguel Hernández de Elche, Alicante, 03202, Spain.

[6] Histological, Cytological and Digitization Studies Platform, Pathology Department, Hospital Verge de la Cinta, Tortosa, 43500, Spain, and Hospital Universitari Joan XXIII, Tarragona, 43005, Spain.

[7] Hospital Universitari de Bellvitge, IDIBELL, and Universitat de Barcelona, Barcelona, 08908, Spain.

[8] Institute of Neuroscience, National Research Council, Padua, 35127, Italy.

[9] Co-senior authors: Sonia Fernández-Veledo and Joan Vendrell.

Corresponding author: Sonia Fernández-Veledo; Institut d'Investigació Sanitària Pere Virgili, C/ Dr. Mallafrè Guasch, 4, 43005, Tarragona, Spain; +34 977 295 800 ext. 3401; sonia.fernandez@iispv.cat.

Conflict of interest: R.N.K is on the scientific advisory board of Novo Nordisk, Biomea, and REDD.

ABSTRACT

Pancreatic β-cell dysfunction is a key feature of type 2 diabetes, and novel regulators of insulin secretion are desirable. Here we report that the succinate receptor (SUCNR1) is expressed in β-cells and is up-regulated in hyperglycemic states in mice and humans. We found that succinate acts as a hormone-like metabolite and stimulates insulin secretion *via* a SUCNR1–Gq-PKC-dependent mechanism in human β-cells. Mice with β-cell-specific *Sucnr1* deficiency exhibit impaired glucose tolerance and insulin secretion on a high-fat diet, indicating that SUCNR1 is essential for preserving insulin secretion in diet-induced insulin resistance. Patients with impaired glucose tolerance show an enhanced nutritional-related succinate response, which correlates with the potentiation of insulin secretion during intravenous glucose administration. These data demonstrate that the succinate/SUCNR1 axis is activated by high glucose and identify a GPCR-mediated amplifying pathway for insulin secretion relevant to the hyperinsulinemia of prediabetic states.

INTRODUCTION

Insulin secretion by pancreatic β-cells is crucial for blood glucose homeostasis and is tightly controlled by a complex network of hormones, nutrients, and neurotransmitters. Impaired β-cell function worsened by the compensatory hyperinsulinemia associated with insulin-resistant states is a key contributing factor of type 2 diabetes (T2D), a major chronic health concern primarily linked to obesity (1–4). Two different pathways are known to interact in β-cells to ensure insulin secretion in response to glucose stimulation. The well-known “triggering” pathway involves the mitochondrial metabolism of glucose, which induces the closure of ATP-sensitive potassium channels and the activation of voltage-gated Ca^{2+} channels, ultimately triggering the exocytosis of insulin granules (5). However, a second or “metabolic amplifying" pathway is necessary for proper insulin secretion response, involving the external replenishment of the Krebs or tricarboxylic acid (TCA) cycle *via* anaplerosis (6), and is distinct to the neurohormonal amplification pathways (e.g., incretin system) that are related to the activation of G protein-coupled receptors (GPCRs) (7). In addition to this dual and hierarchical control of insulin secretion, emerging evidence points to important roles for anaplerotic TCA cycle substrates that act as second messengers in the cytosol to drive insulin granule exocytosis (8). Within this framework, energy metabolites are increasingly recognized as signaling molecules (9).

In recent years, the TCA cycle substrate succinate has become the poster child for the concept that metabolites can have functions beyond energy metabolism. Cytosolic succinate accumulation occurs largely in response to aerobic glycolysis, breakdown of the TCA cycle and anaplerosis (10). Succinate can also be released into the extracellular space by specific plasma membrane transporters (11, 12), where it behaves akin to classical hormones and

cytokines through engagement with succinate receptor 1 (SUCNR1) (10). Additionally, it has long been known that cell-permeable succinate esters are approximately one-third as potent as glucose at stimulating insulin release, and it is hypothesized that the insulinotropic properties of succinate are based on its capacity to increase the production of mevalonate and NADPH (13–16). Succinate might also act as a stimulus-coupling secondary signal for proinsulin biosynthesis independently of insulin secretion (17, 18). Importantly, succinate has been described as the TCA cycle metabolite more closely associated with second-phase insulin secretion (19). Nevertheless, the extramitochondrial and extracytosolic roles of succinate in insulin secretion are unexplored.

SUCNR1 expression has been observed in the pancreas (20, 21) and in human islets (22), indicating a potential instructive role for the succinate/SUCNR1 axis in islet physiology. Elevated circulating levels of succinate and SUCNR1 activation have been traditionally ascribed to hypoxia, tissue damage, and inflammatory processes (23). Correspondingly, SUCNR1 signaling has been primarily linked to pathophysiology, including metabolic disorders such as obesity, diabetes, and non-alcoholic fatty liver disease (24–31). Nonetheless, previous research has also described a transient rise in extracellular succinate during physiological processes, including exercise (12, 32), with which it is involved in muscle innervation and matrix remodeling *via* SUCNR1 (12). Also, we recently demonstrated that dynamic succinate regulation occurs during fasted-to-fed transition, which is potentiated when nutrients are sensed by the intestine but is disturbed in unhealthy metabolic states (33). Therefore, the initial view of SUCNR1 as an exclusive sensor for local damage is being reshaped in the light of recent observations of succinate as a systemic metabolic signal.

SUCNR1 can signal through cAMP- or Ca^{2+}-dependent pathways (34–36), which are well-known regulators of insulin secretion in β-cells (37). Notably, global *Sucnr1*-knockout mice fed high-fat diet (HFD) show defective insulin secretion and glucose intolerance, without significant changes in β-cell mass (25), raising suspicion of its role as a regulator of β-cell function. Here, we adopted a comprehensive and integrative translational approach to investigate the impact of the succinate/SUCNR1 axis on the β-cell function. Our investigation using a unique pancreatic β-cell-specific knockout mouse model and in vitro analyses demonstrates that the succinate/SUCNR1 axis serves a glucose-dependent amplifying transduction pathway enhancing insulin release. Furthermore, we find that succinate functions as an incretin-like metabolite, which significantly potentiates insulin secretion in hyperglycemia in humans.

RESULTS

Pancreatic β-cells express SUCNR1

We first analyzed *Sucnr1* mRNA levels in metabolic tissues from mice (**Figure 1A**), confirming *Sucnr1* expression in the total pancreas, albeit at low levels compared with white adipose tissue and liver, in agreement with previous reports (20, 21, 38). Immunohistochemical staining of pancreas sections revealed a higher SUCNR1 protein abundance in islets than in exocrine tissue in both human and mouse samples (**Figure 1B**). To gain insight into the cell type-specific expression of SUCNR1 in pancreatic islets, we examined its mRNA levels in the two major cell populations: α- and β-cells (39). Results showed that *Sucnr1* was specifically expressed in β-cells from rat islets (**Figure 1C**). Gene expression regulation differs across tissues, and particular factors may influence *SUCNR1* expression in human islets. *In silico* analysis of the human *SUCNR1* gene using the Islet Regulome Browser (40) identified NKX2.2, FOXA2, and NKX6.1 as putative regulators of *SUCNR1* expression, which are key transcription factors for β-cell identity and function (41–43). Bioinformatics analysis also revealed *SUCNR1* expression in a published RNA-seq library from human islets (44). Finally, the *SUCNR1* locus and its surrounding regions contained several single-nucleotide polymorphisms identified in patients with T2D in a genome-wide association study dataset (45) (**Figure 1D**).

SUCNR1 expression in islets is regulated in human obesity and T2D

To evaluate whether *Sucnr1* is regulated in the pancreas in different metabolic states, we first assessed its expression in total pancreas tissue from rodent models of obesity and T2D. We

observed a trend for elevated expression in diet-induced obese (DIO) mice and a further trend increase in expression in diabetic (*db*/*db*) mice (**Figure 2A**). Comparable but significant results were obtained in human pancreatic islets from patients with obesity/T2D in two independent cohorts, without significant changes in the levels of *GLP1R* (**Figure 2B**, donor information in **Supplemental Table 1**). These results were confirmed at the protein level in human islet lysates (**Figure 2C**, donor information in **Supplemental Table 2**). In addition, we found a positive correlation between *SUCNR1* mRNA/protein levels in islets and the body mass index (BMI) of the human donors (**Figure 2D**). Overall, these data indicate that islet SUCNR1 is associated with changes in metabolic status, implying a potential role of this receptor in the pathophysiology of metabolic disorders and T2D.

β-cells sense extracellular succinate and release insulin in a SUCNR1-Gq-PKC-dependent mechanism

We next explored a potential link between hyperglycemia and the succinate/SUCNR1 axis in β-cells. Glucose catabolism increases the intracellular levels of succinate in β-cells through pyruvate oxidation *via* the TCA cycle (46). We observed that high-glucose exposure of mouse-derived β-cell line MIN6 stimulated succinate release to the extracellular medium (**Figure 3A**). As pancreatic β-cells can regulate their behavior in response to glucose, we analyzed *Sucnr1* expression in MIN6 cells cultured at different glucose concentrations, finding that glucose increased *Sucnr1* expression in a dose-dependent manner (**Figure 3B**). This result was confirmed at the protein level in the human β-cell line EndoC-βH1 cultured at increasing glucose concentrations (**Figure 3C**).

Our findings that β-cells might increase their sensitivity to extracellular succinate by increasing SUCNR1 expression in response to glucose in a dose-dependent manner prompted us to investigate whether SUCNR1 activation impacts insulin secretion. We observed that extracellular succinate significantly potentiated (20% increase) glucose-stimulated insulin secretion (GSIS) in MIN6 cells (**Figure 3D**). Even though succinate in culture medium takes an anionic form, and as such is widely considered as non-cell-permeable (16), we also utilized the synthetic SUCNR1 agonist *cis*-epoxysuccinic acid (*c*ESA), which has a lower EC_{50} compared to succinate (47), to exclude any intracellular effects of succinate induced by its uptake into cells *via* dicarboxylic acid transporters (48, 49). Results showed that *c*ESA similarly augmented insulin secretion under high glucose (**Figure 3D)**.

The effect of succinate as an extracellular insulin secretagogue was confirmed in EndoC-βH5 cells which, compared with other commonly used human β-cell lines, do not present limitations regarding the expression of some GPCRs (i.e., GLP1-R) (50, 51). EndoC-βH5 cells showed an increase in insulin secretion when SUCNR1 was activated by both extracellular succinate or *c*ESA under conditions of no glucose (1.5-fold or 1.3-fold increase, respectively) and high-glucose (1.4-fold increase for both) conditions (**Figure 3E**). To further demonstrate that the effect of succinate on insulin release is dependent on its extracellular-driven signaling properties, we co-treated cells with the human-specific SUCNR1 antagonist NF-56-EJ40 (52) during the GSIS assay. Acute receptor antagonism completely blocked succinate-induced insulin secretion in the presence of high-glucose (**Figure 3F**), confirming that the insulinotropic effect of extracellular succinate is dependent on SUCNR1.

We next investigated the underlying mechanism of insulin release by SUCNR1 in β-cells. While SUCNR1 transduction pathways remain largely elusive (53), it is increasingly

recognized that they are cell- and context-dependent. We thus challenged MIN6 cells with succinate or *c*ESA and analyzed several canonical proteins that might integrate GPCR signal transduction. Results of western blotting revealed a succinate-dependent increase in the phosphorylated forms of AKT and the novel and atypical PKCs, PKCδ, and PKCζ, respectively, which was accompanied by the differential phosphorylation of ERK1/2 and p38 MAPK (**Figure 4A**). Concomitant with this activation, there was an increase in phosphorylated CREB and phosphorylated (inactive) GSK-3α/β. As β-cells are sensitive to changes in $[Ca^{2+}]$, we also assessed Ca^{2+} mobilization in MIN6 cells upon SUCNR1 activation using a fluorometric assay to measure real-time changes in intracellular Ca^{2+} ($[Ca^{2+}]_i$). We first challenged low-glucose-cultured MIN6 cells with additive doses of succinate, observing no changes in $[Ca^{2+}]_i$. However, when glucose in the culture medium was increased to 16.7 mM, $[Ca^{2+}]_i$ was progressively mobilized with increasing additions of succinate (ANOVA after glucose addition p=0.0126). As cells were exposed to increasing succinate levels before high-glucose stimulation, we studied the succinate effect on Ca^{2+} mobilization immediately after glucose addition. Notably, we also observed a significant glucose-dependent succinate dose-response on $[Ca^{2+}]_i$ in MIN6 cells at lower extracellular succinate doses, which reached significance at 800 μM succinate (ANOVA after glucose addition p=0.0013) (**Figure 4B**). Expanding upon our analysis of MIN6 cells, we examined the influence of succinate on perifused mouse pancreatic islets. Similarly, succinate exhibited no noticeable impact on $[Ca^{2+}]_i$ when islets were exposed to non-stimulatory glucose concentrations, such as 2.8 mM. Since glucose elicits submaximal to maximal Ca^{2+} responses at 16.7 mM in mouse islets (54), which could complicate further assessments of Ca^{2+} effects, we addressed the impact of succinate on glucose-induced Ca^{2+} signals at 8 mM. As shown in Figure 4C, 8 mM glucose elicited the characteristic initial Ca^{2+} transient followed by oscillations. Notably, the

incorporation of succinate at these conditions augmented the amplitude of these Ca^{2+} oscillations, indicating increased Ca^{2+} mobilization (**Figure 4C**).

Within the framework of neurohormonal amplification pathways, PKC activation is almost universally accepted as a major mechanism of GPCR-stimulated insulin secretion (55, 56). To discern the contribution of this family of serine-threonine kinases to SUCNR1-induced insulin secretion, we treated EndoC-βH5 cells with the pan-PKC inhibitor Gö 6983, finding that it partially blocked insulin release stimulated by succinate in high-glucose conditions (**Figure 4D**). Several G proteins are known to mediate GPCR signaling upon receptor activation (57). Given our finding that PKC signaling is implicated in SUCNR1-induced insulin secretion, we assessed the involvement of Gq, which is situated upstream of PKC (58). We used FR900359 to inhibit Gq activity in EndoC-βH5 cells, observing a complete blockade of succinate-induced potentiation of insulin release (**Figure 4E**). Overall, our data suggest the succinate/SUCNR1 axis is a regulator of insulin secretion in a Gq- and PKC-dependent manner.

Specific β-cell ablation of SUCNR1 induces glucose intolerance due to β-cell impairment

To further study the function of SUCNR1 in pancreatic β-cells in vivo, we generated mice with β-cell-specific *Sucnr1* deletion. We crossed mice carrying a conditional *Sucnr1* loxP-flanked locus (*Sucnr1*$^{fl/fl}$) with knock-in heterozygous transgenic mice in which the Cre recombinase gene is introduced at the initiator codon of the *Ins1* endogenous gene locus (*Ins1*$^{Cre/+}$). Accordingly, *Ins1*$^{Cre/+}$ mice do not show recombination in the brain and have similar glucose homeostasis and body weight gains as wild-type mice (59). The resulting offspring included both control mice (*Ins1*$^{+/+}$ *Sucnr1*$^{fl/fl}$, referred to as *Sucnr1*$^{fl/fl}$ or control mice) and mice with β-cell-specific *Sucnr1* ablation (*Ins1*$^{Cre/+}$ *Sucnr1*$^{fl/fl}$, referred to as *Sucnr1*-βKO mice)

(**Supplemental Figure 1**). These mice were born in a typical Mendelian fashion with no recognizable morphological differences between genotypes (data not shown). Immunohistochemical staining revealed a pronounced decrease in SUCNR1 content within pancreatic islets of *Sucnr1*-βKO mice (**Figure 5A**). No differences between genotypes were evident on a normal control diet (NCD) in terms of body weight, glucose and insulin tolerance, and insulin secretion at 16 and 54 weeks of age (**Supplemental Figures 2 and 3**).

We next challenged control and *Sucnr1*-βKO mice to HFD to investigate whether a diet-induced metabolic stress phenotype existed. We found no differences in body weight between groups after 8 weeks of HFD feeding (**Figure 5B**). Remarkably, *Sucnr1*-βKO mice showed an overall higher diet-induced hyperglycemia than control mice, which was particularly significant in random-fed conditions (**Figure 5C**). Simultaneously, *Sucnr1*-βKO mice showed lower plasma insulin levels, which was also notably significant in random-fed conditions (**Figure 5D**). In a general morphometric examination of the pancreas using H&E staining, we observed a trend towards decreased islet mass in *Sucnr1*-βKO mice compared to control mice (**Figure 5E**). This pattern was also observed in the analysis of β- and α-cell mass by immunofluorescence in an additional cohort of mice **(Figure 5F**). Nonetheless, neither of these trends reached statistical significance.

To question whether specific β-cell disruption of *Sucnr1* affected glucose response in an obesity context, we performed a glucose tolerance test (GTT) in mice fed HFD. To consider potential differences in incretin-induced responses in β-cells, we independently challenged mice to an intraperitoneal GTT (i.p. GTT) and an oral glucose gavage GTT (OGTT). Results showed that the glucose response was higher in *Sucnr1*-βKO mice than in control mice for both tests, which was accompanied by a reduced insulin secretory response. These differences were

not associated with changes in the glucose-associated GLP-1 response in *Sucnr1*-βKO mice on HFD (**Figure 5G**). Likewise, no appreciable changes were observed in insulin sensitivity directly measured by an insulin tolerance test (**Figure 5H**) or indirectly by assessing the homeostasis model assessment index of insulin resistance (**Figure 5I**).

To assess if altered circulating insulin levels stemmed from impaired β-cell function in vivo, we measured insulin secretion in isolated islets from control and *Sucnr1*-βKO mice. Under NCD conditions, islets from control mice demonstrated increased insulin secretion following succinate exposure in contrast to the secretion induced by high glucose alone, a phenomenon that was absent in islets from *Sucnr1*-βKO mice (**Supplemental Figure 2E**). In mice challenged with an HFD, islets from control mice showed enhanced insulin secretion upon SUCNR1 activation with succinate or *c*ESA during high glucose conditions. Conversely, such a response was completely blunted in islets from *Sucnr1*-βKO mice (**Figure 5J**). Altogether, these data demonstrate that SUCNR1 plays an essential role in insulin secretion in vivo, particularly in an obesity context.

Succinate functions as a hormone and is associated with the potentiation of insulin secretion in humans

To explore the physiological significance of succinate as an insulin secretagogue, we investigated the potential link between circulating succinate kinetics and pancreatic β-cell function in response to an OGTT and to an isoglycemic intravenous glucose infusion (IIGI) in a cohort of normal glucose tolerant (NGT) or non-NGT subjects according to the American Diabetes Association criteria (60) (**Figure 6A**, clinical and anthropometric data in **Table 1**). As expected, subjects in the non-NGT group had higher fasting plasma glucose and 2-hour

glucose during the OGTT and were insulin resistant. Accordingly, these patients had higher glucose excursions during both OGTT and IIGI, which were accompanied by higher insulin and C-peptide responses (**Figure 6B**). Analysis of the insulin secretion rate (ISR) revealed no significant differences between groups during fasting, although an upward trend was observed in the non-NGT group (**Figure 6C**). Conversely, stimulated ISR was higher in the non-NGT group during both OGTT and IIGI (**Figure 6D**), which agrees with relative hyperglycemia and the characteristic hyperinsulinemia of insulin-resistant states. These differences were not associated with variations in the estimated β-cell glucose sensitivity (**Figure 6E**). Of note, there was a tendency towards elevated fasting levels of circulating succinate in the non-NGT group when compared to the NGT group (**Table 1**). However, it is important to consider that the control group includes individuals with varying degrees of overweight. This aspect may contribute to the observed trend not reaching statistical significance, potentially masking the differences previously reported in subjects with obesity (61, 62). No differences were found between groups in terms of the GLP-1 response (a recognized factor of the amplifying pathway) to the glucose challenge, independently of the route of glucose administration (**Figure 6F**), or the total incretin effect (**Table 1**). Strikingly, however, the succinate response to glucose, which was found higher after nutrient passage through the gut (similar to GLP-1), was significantly higher in the non-NGT group than in the NGT group (**Figure 6G**).

According to the GLP-1 response (**Figure 6F**), incretin potentiation was similar between groups during the OGTT (p=0.7118) (**Figure 6H**). Contrastingly, during the IIGI, in which the incretin effect is considered negligible, the curve of glucose-induced potentiation exhibited a modest decrease in NGT individuals, while conversely, there was a slight increase in non-NGT individuals over time (p<0.0001) (**Figure 6I**). To determine whether succinate is associated with insulin secretion potentiation, we performed a correlation analysis between the

potentiation ratio and the succinate response during the IIGI. A significant correlation between both variables was observed (**Figure 6J**). Overall, this analysis indicates that succinate is associated with insulin secretion in humans, which may be particularly relevant for the hyperinsulinemia developed in insulin-resistant states.

DISCUSSION

Our study uncovers what we consider to be a hitherto unknown molecular link between the succinate/SUCNR1 axis and β-cell function. While previous research in this area primarily focused on the ability of cell-permeable succinate analogs to stimulate insulin secretion through TCA cycle-anaplerosis (13–16), our findings reveal that beyond its intracellular functions, extracellular succinate stimulates insulin secretion in hyperglycemic states in mice and humans *via* SUCNR1 activation. This mechanism represents a significant amplifying pathway for insulin secretion, which may be relevant in prediabetic states where the oversecretion of insulin is an adaptive response to overcome insulin resistance.

Several GPCR-mediated mechanisms cooperate in β-cells to regulate insulin secretion (63). Our study establishes that SUCNR1 in β-cells potentiates insulin secretion in response to high glucose levels, similar to incretins such as GLP-1 and GIP (64). Notably, in humans, we also observed this stimulatory effect on insulin secretion under non-glucose conditions, consistent with previous findings indicating species-specific variations in insulin secretion mechanisms to meet specific physiological needs (65, 66). With regards to the transduction pathways underlying this insulinotropic effect, SUCNR1 signaling differs among cell types (53), but with a preference to engage Gi or Gq proteins (36, 67). We identified a Gq- and PKC-dependent mechanism linking SUCNR1 activation to the potentiation of insulin secretion. Some studies have speculated that increases in $[Ca^{2+}]_i$ observed upon SUCNR1 activation (which we also observed in β-cells) are mediated by Gi and βγ-subunit-induced PLC-β activation rather than Gq (68, 69), but recent studies have established that Gq engagement is required for PKC and $[Ca^{2+}]_i$-mediated responses upon SUCNR1 activation in immune cells (36, 70). Likewise, other

GPCRs such as GPR40 (activated by free fatty acids) have been reported to use pathways mediated by Gq, PKC, and $[Ca_{2+}]_{i,}$ which are known to trigger insulin secretion (71, 72).

Our findings identify the succinate/SUCNR1 axis as an amplifying route for insulin secretion in response to hyperglycemia. Indeed, high glucose significantly increases β-cell sensitivity to extracellular succinate by elevating SUCNR1 expression. Accordingly, SUCNR1 expression is significantly greater in islets from donors with obesity and T2D than in lean control donors, which fits with our previous findings of higher circulating succinate levels in the former (61, 62). The upregulation of SUCNR1 associated with hyperglycemia differs, however, from the downregulation reported for GLP1-R in conditions associated with high glucose (73, 74). Notably, several identified risk variants for T2D have been mapped at the *SUCNR1* locus or are in close proximity to *cis*-regulatory elements (40, 42, 75). Collectively, these findings might suggest that modifications in SUCNR1 expression in β-cells in some diseases are linked to metabolic cellular adaptations and an elevated risk of developing T2D.

SUCNR1 activation is traditionally recognized as a mechanism bolstering tissue damage (76–81). Indeed, chronic elevation of extracellular succinate is found in low-grade inflammatory metabolic disorders such as cardiovascular disease, obesity, and T2D (26, 61, 82, 83). However, circulating succinate levels also rise transiently in response to normal physiological processes such as exercise (12) and food intake (33). The nutritional regulation of succinate is dependent on glucose sensing by the intestine and the metabolic status of the subject (33), suggesting a key signaling role for succinate for metabolic processes related to energy management (10). Along this line, we recently showed that the succinate/SUCNR1 axis is a regulator of leptin production in adipocytes (84). This study, in addition to our current findings identifying a function for succinate as an insulin secretagogue, strongly supports a role for

SUCNR1 as part of the metabolite-sensing machinery allowing cells to coordinate energy homeostasis. Consistent with this hypothesis, we show that β-cell specific depletion of SUCNR1 in mice leads to an aberrant metabolic phenotype characterized by increased glucose intolerance and defects in insulin secretion under HFD feeding. While there is a discernible trend towards reduced β-cell mass in *Sucnr1*-βKO mice under HFD conditions, suggesting a potential impact of SUCNR1 on β-cell proliferation, it is important to note that this change lacks statistical significance. As a result, we propose that SUCNR1 exerts its primary influence on the functionality of adult β-cells, rather than on their development or the typical compensatory alterations in β-cell mass observed during obesity (85). The observed similarities in the GLP-1 response between *Sucnr1*-βKO mice and control mice on an HFD, coupled with the pronounced impairment in insulin secretion and glucose tolerance in the *Sucnr1*-βKO mice, underscores the pivotal role of SUCNR1 in preserving insulin secretion. Despite the absence of incretin response both in *Sucnr1*-βKO mice and control mice in diet-induced obesity, β-cells in *Sucnr1*-βKO mice fall short in counteracting hyperglycemia, which emphasizes the critical involvement of the succinate-SUCNR1 axis in this scenario. Moreover, our findings align with an earlier study using global *Sucnr1* knockout mice, which exhibited progressive glucose intolerance under HFD and an impaired insulin response, occurring as part of a complex phenotype (25). However, other organs (e.g., adipose tissue) also influence these phenotypes, underscoring the importance of analyzing the effects of SUCNR1 in specific cell types (10, 24, 84).

Our study in patients highlights the significance of the succinate/SUCNR1 axis in preserving glucose homeostasis during metabolic challenges. Prediabetes, a state observed in non-normal glucose tolerant (non-NGT) patients, is characterized by glucose intolerance resulting from systemic insulin resistance, which is substantially compensated for by the oversecretion of

insulin (86) through mechanisms that remain elusive. When challenged with glucose, we observed a transient increase in succinate levels following glucose administration, particularly elevated in prediabetic individuals, while the GLP-1 response mirrored that of subjects with NGT. This suggests that factors beyond incretins may play a role in modulating the enhanced insulin secretion seen in prediabetic conditions. In this context, succinate emerges as a regulator of the observed hyperinsulinemic response in prediabetic patients. No significant differences in incretin-related potentiation were observed between the groups during an OGTT, likely due to preserved operation of the incretin system in patients with non-NGT. However, during intravenous glucose infusion, where the incretin effect on insulin secretion is negligible (87), we found a positive correlation between the succinate response and insulin secretion potentiation. The succinate response to glucose is higher during –but not exclusive to– the oral challenge (33), which prompts the consideration of other succinate sources in addition to the intestine. We observed that β-cells secrete more succinate when they are exposed to high glucose, which is consistent with previous studies showing that hyperglycemia can also lead to local increases in succinate (80, 88), likely due to overactivation of the TCA cycle (89). Thus, it is tempting to speculate that succinate endogenously produced in β-cells could be partly responsible for SUCNR1 engagement in an autocrine fashion. Succinate derived from the gut microbiota is also a potential source (10), and indeed, other metabolites derived from the gut microbiota, including short-chain fatty acids, have been described as insulin secretagogue GPCR ligands (90, 91).

While the human study offers valuable associative insights, the concurrent presence of heightened glucose intolerance, insulin secretion, and succinate response in prediabetic conditions prevents us from conclusively establishing a direct link between the succinate/SUCNR1 axis and insulin secretion. However, our integrated findings encompassing

patient observations and preclinical models collectively suggest that the succinate/SUCNR1 axis in β-cells intricately regulates insulin secretion and helps maintain glucose homeostasis, particularly under metabolic stress conditions. The observed upregulation of SUCNR1 in human islets during obesity and diabetes, coupled with evidence from our β-cell SUCNR1 knockout model, point to a compensatory mechanism aimed at counteracting metabolic challenges.

Our findings highlight SUCNR1 as a potential therapeutic target to enhance insulin secretion in the context of T2D management. Indeed, the nutritional modulation of succinate is lost in patients with morbid obesity and T2D (33). Nonetheless, further research is needed due to the broad expression of SUCNR1 and its pleiotropic functions (10). While the succinate/SUCNR1 axis is crucial for the resolution of inflammation (24, 36), activation of SUCNR1 in an inflammatory context could be detrimental due to its pro-inflammatory effects in the acute phase of the immune response (78, 92). Along these lines, decreasing the higher levels of circulating succinate acting on its intestinal source, rather than directly activating SUCNR1, has recently emerged as a potential strategy for treating metabolic diseases (93). Whether this strategy could also be effective in recovering the function of SUCNR1 on insulin secretion deserves further analysis.

METHODS

Sex as a biological variable

In human studies, we included both male and female individuals. Sex was consistently considered as a variable, yet no differences were detected. In animal studies, we exclusively examined male animals. The relevance of our findings to female animals is unknown, despite observing no sex-dependent differences in humans.

Human cohort

The study was carried out at the Unit of Functional Studies, Institut d'Investigació Sanitària Pere Virgili, Hospital Universitari Joan XXIII, Tarragona, Spain. As part of a screening protocol for obesity in the general population, healthy asymptomatic subjects were selected from those who visited the Endocrinology Service. The main inclusion criteria were as follows: age between 18-65 years, BMI < 35 $kg \cdot m^{-2}$; absence of underlying pathologies (cancer, liver disease, kidney disease, or systemic inflammation) on physical examination, diagnostic tests other than those associated with an excess of weight; and signing the protocol-informed consent. Additionally, inclusion criteria required a level of HbA1c < 6.5% and a fasting glucose level < 126 $mg \cdot dl^{-1}$ in two separate occasions. After the initial triage, thirty subjects were selected to be submitted to an oral glucose tolerance test (OGTT) with 75 g of glucose. Individuals were classified according to the American Diabetes Association (ADA) criteria (60) as normal glucose tolerant (NGT; fasting glucose levels ≤ 110 $mg \cdot dl^{-1}$ and a normal OGTT response) or non-NGT (fasting glucose levels ≥ 110 and < 126 $mg \cdot dl^{-1}$, or impaired glucose tolerance or diabetes during an OGTT following the ADA criteria) (clinical information

summarized in **Table 1**). The main exclusion criteria were pregnancy and lactation; vegetarianism, veganism, or eating disorders; chronic treatment with anti-inflammatory agents, antibiotics, or cortisol; and major psychiatric antecedents, alcoholism, or drug abuse.

Assessment of β-cell function and succinate dynamics in humans

All participants underwent two procedures on separate occasions. First, we applied a 3-hour OGTT and subsequently a 3-hour intravenous isoglycemic glucose infusion (IIGI), reproducing the plasma glucose time curve recorded during the OGTT using an *ad hoc* algorithm. Plasma glucose was determined every ten minutes during both procedures, whereas insulin, C-peptide, GLP-1, and succinate were determined in plasma samples at -30, 0, 10, 20, 30, 60, 90, 120, 150, and 180 minutes. Body composition was determined by electric bioimpedance (Tanita Europe BV; Amsterdam, The Netherlands). During blood collection, a specific DPP-IV inhibitor was present in the tubes (DPP4-010; Merck KGaA, Darmstadt, Germany). Blood samples were always kept on ice and stored at -80 ºC. Plasma lipid, hepatic and renal profiles were determined by standard enzymatic methods. Plasma glucose was determined by the glucose oxidase method (GM-9; Analox, London, UK). Plasma insulin and C-peptide levels were determined by an immunochemiluminometric assay (ADVIA Centaur; Siemens Healthcare, Erlangen, Germany). Total plasma GLP-1 levels (7-36 and 9-36) were determined by ELISA (EZGLP1T-36 K; Merck). Plasma succinate was determined in plasma filtrates (10 kDa) using a fluorometric assay (EnzyChrom Succinate Assay Kit; BioAssay Systems, Hayward, CA).

The areas under the curve (AUC) were calculated using the trapezoid rule. Insulin sensitivity was estimated from the plasma glucose and insulin responses to oral glucose using the OGTT-

derived index of insulin sensitivity (OGIS) (94). In vivo insulin secretion, β-cell function parameters, and the incretin effect were calculated by simultaneous modeling analysis of the IIGI and the OGTT, as previously described (95). The model reconstructs insulin secretion from plasma C-peptide using an established model of C-peptide kinetics (96) and it extends a widely used model for the analysis of the OGTT (97). In brief, the model describes the relationship between insulin secretion and glucose concentration during the IIGI as a quasi-linear function (i.e., the dose-response). This response is modulated during the test by a time-dependent factor, which averages to one. This time-dependent factor, denoted as glucose-induced potentiation, accounts for potentiation phenomena that typically prompt glucose-dependent insulin secretion higher at the end of the test compared to the beginning. The model also includes a term describing early secretion, related to first-phase insulin release. Insulin secretion during the OGTT is described by the same terms, although the dose-response is multiplied by another time-dependent factor, typically greater than one, which accounts for the effect of incretin hormones on insulin secretion. This time-dependent factor is denoted incretin potentiation, and its AUC is a measure of the total incretin effect. To study a potential relationship between the insulin secretion potentiation during the IIGI and succinate dynamics, we used the potentiation ratio between 2 hours and the baseline, and the corresponding 2-hour incremental succinate AUC mean.

Animals

Male Wistar rats (Charles River Laboratories, Wilmington, MA) were housed in the Animal Facility of Miguel Hernández University. All mice were housed in the Animal Facility of the Faculty of Medicine and Health Sciences, Universitat Rovira i Virgili. Housing conditions consisted of automated 12-h light-dark cycles at 20-22 ºC, 40-60% relative humidity, and *ad*

libitum access to NCD (3.1 kcal% fat; SAFE Diets, A04) or HFD (60 kcal% fat; Research Diets Inc., D12492). HFD availability to mice started at 8 weeks of age until the study endpoint. Male mice were weighed prior to any experimental procedure. At the end of the study, mice were fasted for 16 h and then euthanized by cervical dislocation. Tissues were collected and immediately snap-frozen in liquid N_2 or fixed in 4% formaldehyde.

Male wildtype C57BL/6 mice and male diabetic *db*/*db* mice were obtained from Charles River Laboratories. β-cell specific *Sucnr1* knockout mice (*Sucnr1*$^{fl/fl}$ *Ins1*$^{Cre/+}$, *Sucnr1*-βKO) were obtained in the F2 generation by crossing parental homozygous *Sucnr1* floxed mice (*Sucnr1*$^{fl/fl}$ *Ins1*$^{+/+}$, control) (24) and *Ins1*$^{Cre/+}$ mice, the latter kindly provided by J. Ferrer (Centre for Genomic Regulation, Barcelona, Spain). Briefly, *Ins1*$^{Cre/+}$ mice were generated by a knock-in strategy into one endogenous *Ins1* allele and present more specificity for restricted β-cell Cre expression, avoiding recombination in other tissues, including the brain (59). Control Cre-negative mice were generated in the same litters along with *Sucnr1*-βKO mice (**Supplemental Figure 1**). All resulting mice were generated on a pure C57BL/6 background and genotyped by PCR using specific primers to amplify *Sucnr1*$^{+}$ and *Sucnr1*^{fl} alleles (300 bp product for the wild-type allele and 450 bp product for the floxed form) and to amplify *Ins1*$^{+}$ or *Ins1*^{Cre} alleles (524 bp for the wild-type and 865 bp for the mutated structure).

Physiological experiments on mice

For the i.p. and oral GTT, 16- and 54-week-old male mice were fasted for 16 h, and blood glucose was measured before and 15, 30, 60, and 120 min after administration of glucose (2 g·kg^{-1} body weight). For the ITT, male mice were fasted for 4 h, and blood glucose was measured before and 15, 30, 60, and 120 min after an i.p. injection of recombinant human

insulin (0.75 IU·kg^{-1} body weight; Actrapid, Novo Nordisk, Denmark). Blood glucose was measured using a glucose meter (Accu-Chek; Roche). The area under the curve for glucose was calculated using the trapezoidal rule for any tolerance test (98). Plasma insulin was determined using a Mouse Insulin Ultrasensitive ELISA kit (Mercodia, Uppsala, Sweden). GLP-1 levels were analyzed in plasma using a Mouse GLP-1 ELISA kit (Crystal Chem, Elk Grove Village, IL).

Cell lines

EndoC-βH1 is an engineered cell line obtained from a male human pancreas subjected to lentiviral transfection of the SV40 large T antigen (SV40LT) expressed under the control of the insulin promoter and the human telomerase reverse transcriptase (hTERT) (99). These cells present several similarities to primary human β-cells (100). EndoC-βH1 cells were cultured as described (101). Briefly, before seeding the cells, the culture dishes and plates were coated with a mixture of DMEM (4.5 g·l^{-1} glucose; Thermo Fisher Scientific, Waltham, MA), fibronectin (2 µg·ml^{-1}; Thermo Fisher Scientific), and extracellular matrix (1%; Sigma-Aldrich, Saint Louis, MO). The coated flasks were then incubated for at least 1 hour in a 5% CO_2 atmosphere at 37 °C. EndoC-βH1 cells were maintained at 37 ºC and 5% CO_2 in DMEM-based media consisting of 1 g·l^{-1} glucose, 2% BSA, 50 µM 2-mercaptoethanol (Sigma-Aldrich), 10 mM nicotinamide (Sigma-Aldrich), 5.5 µg·ml^{-1} transferrin (Sigma-Aldrich), 6.7 ng·ml^{-1} sodium selenite (Sigma-Aldrich), and 1% penicillin-streptomycin (Thermo Fisher Scientific). To measure SUCNR1 protein levels, cells were starved for 16 h in 2.8 mM glucose DMEM-based media followed by treatment with 5.5, 11.1, 16.7, or 25 mM glucose for 24 h.

The latest iteration of the human EndoC cell series is the EndoC-βH5 cell line, which was purchased from Human Cell Design (Toulouse, France). These cells are derived from human female fetal pancreatic tissue and demonstrate an improved insulin secretion response, heightened sensitivity to incretins, and more pronounced expression of β-cell identity markers in comparison with other human β-cell lines, displaying a greater similarity to primary adult β-cells. The generation process of these cells was similar to previous models, but the SV40LT, hTERT, and herpes simplex virus-1 thymidine kinase transgenes were removed through Cre-mediated recombination to produce mature, non-proliferative cells (51). EndoC-βH5 cells were seeded at 1×10^5 cells per well in βCOAT matrix (Human Cell Design) pre-treated 96-well Cell$^+$ plates (Sarstedt, Nümbrecht, Germany) and cultured for 10 days prior to performing the GSIS assays. Cells were maintained in ULTI-β1 medium (Human Cell Design), and the medium was changed 4 hours after seeding, when all viable cells had attached, and then again 4 days later.

MIN6 is an insulinoma-derived cell line from transgenic male mice transfected with SV40 T-antigen, with the ability to secrete insulin in the presence of glucose. MIN6 cells were maintained under standard culture conditions (102). Briefly, MIN6 cells were cultured at 37 ºC and 5% CO_2, in DMEM consisting of 4.5 $g\cdot l^{-1}$ D-glucose, 2 mM L-glutamine (Thermo Fisher Scientific), 15% fetal bovine serum (Thermo Fisher Scientific), 1% penicillin-streptomycin, 20 mM HEPES (Thermo Fisher Scientific), and 50 µM 2-mercaptoethanol. To assess *Sucnr1* gene expression levels, cells were starved for 16 h in 2.8 mM glucose DMEM-based media followed by stimulation with 5.5, 11.1, or 16.7 mM glucose for 3 and 24 hours.

Gene expression analysis

RNA was extracted from tissues or cells using TRIzol Reagent and cDNA was synthesized using the High-capacity cDNA Reverse Transcription kit (both from Thermo Fisher Scientific). Quantitative real-time PCR amplification was performed on a 7900HT Fast Real-Time PCR System with the TaqMan Gene Expression Assay from Thermo Fisher Scientific (probes are listed in **Supplemental Table 3**). Relative mRNA levels were calculated using the comparative $2^{-\Delta\Delta Ct}$ method, corrected for the corresponding housekeeping gene expression levels, and displayed as Log2 for normalization.

Western blotting

Cells or tissues were lysed in M-PER buffer containing Halt Protease and Phosphatase Inhibitor Cocktails and protein concentration was measured using the BCA protein assay kit (all from Thermo Fisher Scientific). Samples were resolved on SDS-PAGE gels and proteins were transferred onto PVDF membranes (Merck KGaA, Darmstadt, Germany). Membranes were blocked in a blocking buffer consisting of 5% blotting-grade blocker non-fat dry milk (Bio-Rad, Hercules, CA) and incubated with primary antibodies overnight at 4°C. A polyclonal primary antibody against SUCNR1 (NBP1-0086) was obtained from Novus Biologicals (Centennial, CO). A monoclonal anti-β-actin antibody was purchased from Sigma-Aldrich (A1978). Primary antibodies against phospho-PKCδ (T505) (#9374), phospho-PKCζ/λ (T410/403) (#9378), phospho-Akt (S473) (#4058), phospho-GSK-3α/β (S21/9) (#9331), phospho-ERK1/2 (T202/Y204) (#9101), phospho-p38 (T180/Y182) (#4511), and phospho-CREB (S133) (#9198) were obtained from Cell Signaling Technology (Danvers, MA). Membranes were incubated with the respective HRP-linked secondary antibodies for 1 h and

developed using the Pierce ECL Western Blotting Substrate or SuperSignal West Femto Maximum Sensitivity Substrate (Thermo Fisher Scientific). Band intensity was captured using the iBright CL1000 Imaging System and analysis was performed with the iBright Analysis Software (Thermo Fisher Scientific).

Glucose-stimulated insulin secretion assays

MIN6 cells were washed twice in Krebs-Ringer-Phosphate-HEPES (KRPH) buffer (5 mM Na_2HPO_4, 1 mM $MgSO_4$, 1 mM $CaCl_2$, 136 mM NaCl, 4.7 mM KCl, 20 mM HEPES pH 7.4, and 0.5% BSA), incubated in KRPH buffer with 2.8 mM D-glucose for 1 h at 37 ºC, 5% CO_2 and saturated humidity, and then washed twice with KRPH buffer. Cells were then incubated for 1 h in KRPH buffer containing either 2.8 or 16.7 mM D-glucose and the corresponding stimulus. EndoC-βH5 cells were subjected to GSIS assays following the manufacturer's protocol (Human Cell Design). In brief, cells were starved in ULTI-ST medium for 24 hours, then washed twice in βKrebs medium (both from Human Cell Design) supplemented with 0.1% BSA (βKrebs-BSA) and incubated in βKrebs-BSA medium for 1 h at 37 °C, 5% CO_2 and saturated humidity. Cells were then stimulated for 40 min with 0 or 20 mM glucose and the indicated stimulus in βKrebs-BSA media. At the end of GSIS assays, the CM from cells was collected and centrifuged at 300 RCF for 15 min at 4 ºC, and the supernatant was stored at -80 ºC. The remaining cells or islets were washed once in PBS and lysed with M-PER buffer with Halt Protease Cocktail (Thermo Fisher Scientific) for protein quantification.

Pools of 300 islets (100 islets per mouse) were pre-incubated with Krebs-Ringer-Bicarbonate-HEPES (KRBH) buffer, consisting of 115 mM NaCl, 2.5 mM $CaCl_2 \cdot 2H_2O$, 24 mM $NaHCO_3$, 5 mM KCl, 1 mM $MgCl_2 \cdot 6H_2O$, 20 mM HEPES, and 0.5% BSA, pH 7.4, and containing 2.8

mM glucose at 37 °C and 5% CO_2 for 2 hours. Subsequently, sets of 10 islets per condition, in quintuplicates, were incubated in KRBH buffer with either 2.8 mM or 16.7 mM glucose, with or without the addition of the indicated stimuli. After 1 hour, the CM from islets was collected, centrifuged at 300 RCF for 15 minutes at 4 °C, and the supernatant was then stored at -80 °C. Total insulin contents were extracted using a lysis buffer composed of 5.75% acetic acid (Sigma-Aldrich) and 0.1% BSA.

Reagents for GSIS assays were 0.5–1 mM disodium succinate (W327700; Sigma-Aldrich), 50-100 µM *cis*-epoxysuccinic acid (*c*ESA; E0449; TCI Chemicals, Tokyo, Japan), 1 µM NF-56-EJ40 (HY-130246; MedChemExpress, Monmouth Junction, NJ), 1 µM Gö 6983 (#2285, Tocris, Bristol, UK), and 1µM FR900359 (#33666, Cayman Chemical Co., Ann Arbor, MI). Inhibitors were pre-incubated for 3 h in all media preparations during the assays at the reported concentrations. The insulin content in the CM and lysates was measured using Mouse or Human Insulin ELISA kits (Mercodia).

Measurement of cytosolic Ca^{2+}

Intracellular free Ca^{2+} was determined in MIN6 cells grown on glass coverslips (Menzel-Gläser, Germany). At 80% confluency, the coverslip was carefully transferred to a Petri dish containing 3 ml of Locke-HEPES buffer (LH) comprising 120 mM NaCl, 10 mM KCl, 15 mM $NaHCO_3$, 3.3 mM $MgCl_2$, 2.6 mM $CaCl_2$, 2.8 mM D-glucose and 10 mM HEPES, pH 7.4 and including 6 µM Fura-2-acetoxymethyl ester (Fura-2-AM; Thermo Fisher Scientific). Cells were incubated at 37°C for 30 min in a cell incubator. For fluorescence recordings, the coverslip was carefully rinsed in LH, mounted in a specific holder (coverslip accessory L2250008; PerkinElmer, Waltham, MA), and placed in a quartz cuvette containing 1.3 ml of

LH buffer. Measurements were made at 37°C with continuous mild stirring in an LS50B PerkinElmer fluorescence spectrometer equipped with a fast-filter accessory for Fura-2 fluorescence ratio measurements. Emission data (510 nm) were collected with alternate excitation at 340 and 380 nm and the ratio F_{340}/F_{380} was calculated in real-time using proprietary software (FL WinLab 2.0; PerkinElmer). The mobilization of cytosolic Ca^{2+} by extracellular succinate was evaluated before and after the increase of glucose to 16.7 mM.

Ca^{2+} measurements were also performed in isolated islets from 12-week-old male mice. After isolation, islets were allowed to recover for 2 hours at 37 ºC and then incubated with 2 µM Fura-2-AM at room temperature. Then, islets were transferred to an imaging chamber mounted on a Zeiss Axiovert 200 inverted microscope (Zeiss, Jana, Germany) equipped with a 40X objective. During experiments, islets were continuously perifused with a KRBH buffer (pH=7.35) containing the corresponding stimuli. Images were acquired using a Hamamatsu C9100 digital camera (Hamamatsu Photonics, Hamamatsu, Japan). Intracellular Ca^{2+} levels were represented as the ratio F_{340}/F_{380}. The AUC at 8 mM glucose was calculated for 5 minutes before the application of succinate. The AUC of succinate was also calculated for 5 minutes, but 10 minutes after succinate application to allow its equilibration in the perifusion chamber.

Statistical analysis

The data presented in tables and graphics are displayed as either the mean ± SD or mean ± SEM, as indicated. In the box-and-whisker plots, the median is indicated by a center line, while the upper and lower quartiles are represented by the box limits, and the minimum to maximum range of the data set is indicated by the whiskers. The Shapiro-Wilk normality test was applied before any contrast hypothesis testing. When the data were normally distributed, a two-tailed

Student's *t*-test was used to compare differences between two groups, applying Welch's correction if a difference between the variations of the compared groups was observed. For comparisons involving multiple groups, a one-way ANOVA was performed; Dunnett's *post hoc* test was used when comparing multiple groups to a control group, while Tukey's *post hoc* test was applied for comparing all groups with each other, to correct for multiple comparisons. For time-course experiments, a two-way ANOVA with Bonferroni's correction for multiple comparisons were conducted. In cases where the data did not follow a normal distribution, the non-parametric Mann-Whitney two-tailed *U*-test for unmatched pairs, the Wilcoxon signed-rank test for matched pairs, or the Kruskal-Wallis test with Dunn's test for multiple comparisons were used to compare differences as appropriate. Pearson's or Spearman's correlations were employed to calculate linear associations between continuous variables. Both GraphPad Prism 9 and RStudio software for Mac OS and IBM SPSS 27 software for Windows OS were utilized for the statistical analyses, and a *p*-value of less than 0.05 was considered statistically significant.

Study approval

The conduct of the study protocols was in accordance with the ethical principles outlined in the Declaration of Helsinki and received authorization from the relevant local ethics committees (IISPV Ethics Research Committee reference number 204/2017). Prior to their participation, all subjects were given a thorough explanation of the study protocol and provided written informed consent.

The use of human islets for gene expression analysis was approved by the local Ethics Committee of Hospital Universitari de Bellvitge (approval PR239/13), and signed consent was

obtained from donor relatives. All studies and protocols involved in human islet procurement and experimentation (for the protein expression analysis) were approved by the Joslin Diabetes Center's Committee on Human Studies (approval CHS#5-05).

All animal studies conformed to the ARRIVE guidelines and were carried out under the supervision and approval of the Animal Welfare and Governmental Ethics Committee of the Universitat Rovira i Virgili (project reference number 10970). All experimental procedures involving animals conformed to the European Union Directive 2010/63/EU and the European Commission Recommendation 2007/526/EC on the protection of animals used for experimental and other scientific purposes, enacted under the Spanish Royal Decrees 53/2013 and 118/2021.

Data availability

Further information is available in Supplemental Methods, which is included in the **Supplemental Data** document. All data points presented in the graphs are detailed in the **Supporting Data Values** file.

AUTHOR CONTRIBUTIONS

Conceptualization was the responsibility of J.S.B., B.A., J.V., and S.FV.; Methodology was the responsibility of J.S.B., B.A., C.C., M.E., J.B., M.R.D.D., I.Q., D.F.D.J., L.M., R.B., and F.S.; Formal Analysis was conducted by J.S.B., B.A., J.B., F.S., A.T., and A.M.; Investigation was conducted by J.S.B., B.A., C.C., M.E., M.R.D.D., I.Q., J.B., C.N.R., L.M, D.F.D.J., L.M., and R.B.; Resources were provided by L.M., A.T., A.M., and R.N.K.; Original draft writing was conducted by J.S.B.; Manuscript review and editing was the responsibility of J.S.B., A.T., A.M., R.N.K, J.V., and S.FV.; Supervision was carried out by J.V. and S.F.V.; Funding was acquired by J.V. and S.F.V.

ACKNOWLEDGEMENTS

This research was supported by grants RTI2018-093919-B-100 and PID2021-122480OB-I00 (to S.F.V), PID2020-118127RB-I00 (to F.S.), and PID2020-117569RA-I00 (to L.M.) from the Spanish Ministry of Science and Innovation (MCIN; MCIN/AEI/10.13039/501100011033) and by the European Regional Development Fund (ERDF), "ERDF, A way of making Europe". This research also received funding from "La Caixa" Foundation (ID 10001 0434) under the grant agreement LCF/PR/HR20/52400013 (to S.F.V.), the Catalan Association of Diabetes, and from the Instituto de Salud Carlos III (PI20/00338 to J.V. and PI19/00246 to E.M.), co-financed by the ERDF and from CIBER-Consorcio de Investigación Biomédica en Red (CB07708/0012), Instituto de Salud Carlos III, MCIN. J.S.B. is a recipient of a PhD Fellowship in Biomedical Research from the Instituto de Salud Carlos III and MCIN, co-founded by the European Social Fund (FI18/00151). B.A. is a recipient of a contract from the PERIS Program of the Generalitat de Catalunya (SLT017/20/000033). C.C. acknowledges support from the

“Juan de la Cierva” track program (FJC2021-047047-I), from the MCIN, AEI, and NextGenerationEU. M.R.D.D. is a recipient of a grant from the “Martí i Franquès” Research Program from Universitat Rovira i Virgili (2021PMF-PIPF-2). M.M.R.P. is a recipient of a contract from the PERIS program of the Generalitat de Catalunya (SLT/028/23/000013). D.F.D.J. acknowledges support by Mary K. Iacocca Junior Postdoctoral Fellowship and the American Diabetes Association (grant 7-21-PDF-140). S.F.V. and J.V.O. acknowledge support from the Agency for Management of University Research Grants of the Generalitat de Catalunya (2021-SGR-1409 and 2021-SGR-829). S.F.V. acknowledges support from the Miguel Servet Tenure-Track Program (CP10/00438 and CPII16/00008) from the Fondo de Investigación Sanitaria, co-funded by the ERDF. R.N.K. acknowledges support from the National Institutes of Health (grant R01 DK067536). We would like to express particular gratitude to the patients and the IISPV BioBank (PT17/0015/0029), integrated in the Spanish National BioBank Network (#C.0003609), for their collaboration. We thank Dr. Jorge Ferrer for kindly providing the transgenic mice expressing the Cre recombinase within the *Ins1* gene and Dr. Kenneth McCreath for his helpful comments on the manuscript.

REFERENCES

1. Wahl S, et al. Epigenome-wide association study of body mass index, and the adverse outcomes of adiposity. *Nature*. 2017;541(7635):81–86.
2. Cerf ME. Beta cell dysfunction and insulin resistance. *Front Endocrinol (Lausanne)*. 2013;4:37.
3. Fonseca VA. Defining and characterizing the progression of type 2 diabetes. *Diabetes Care*. 2009;32 Suppl 2(Suppl 2):S151-6.
4. Shigeta H, et al. Lifestyle, Obesity, and Insulin Resistance. *Diabetes Care*. 2001;24(3):608–608.
5. Rorsman P, Ashcroft FM. Pancreatic β-Cell Electrical Activity and Insulin Secretion: Of Mice and Men. *Physiol Rev*. 2018;98(1):117–214.
6. Alves TC, et al. Integrated, Step-Wise, Mass-Isotopomeric Flux Analysis of the TCA Cycle. *Cell Metab*. 2015;22(5):936–947.
7. Kalwat MA, Cobb MH. Mechanisms of the amplifying pathway of insulin secretion in the β cell. *Pharmacol Ther*. 2017;179:17–30.
8. MacDonald MJ, et al. Perspective: emerging evidence for signaling roles of mitochondrial anaplerotic products in insulin secretion. *Am J Physiol Endocrinol Metab*. 2005;288(1):E1–E15.
9. Martínez-Reyes I, Chandel NS. Mitochondrial TCA cycle metabolites control physiology and disease. *Nat Commun*. 2020;11(1):102.
10. Fernández-Veledo S, Ceperuelo-Mallafré V, Vendrell J. Rethinking succinate: an unexpected hormone-like metabolite in energy homeostasis. *Trends Endocrinol Metab*. 2021;32(9):680–692.

11. Prag HA, et al. Mechanism of succinate efflux upon reperfusion of the ischaemic heart. *Cardiovasc Res*. 2021;117(4):1188–1201.

12. Reddy A, et al. pH-Gated Succinate Secretion Regulates Muscle Remodeling in Response to Exercise. *Cell*. 2020;183(1):62-75.e17.

13. Attali V, et al. Regulation of insulin secretion and proinsulin biosynthesis by succinate. *Endocrinology*. 2006;147(11):5110–5118.

14. Henquin J-C, Dufrane D, Nenquin M. Nutrient control of insulin secretion in isolated normal human islets. *Diabetes*. 2006;55(12):3470–7.

15. Maechler P, et al. Mitochondrial activation directly triggers the exocytosis of insulin in permeabilized pancreatic beta-cells. *EMBO J*. 1997;16(13):3833–41.

16. MacDonald MJ, et al. Effect of esters of succinic acid and other citric acid cycle intermediates on insulin release and inositol phosphate formation by pancreatic islets. *Arch Biochem Biophys*. 1989;269(2):400–6.

17. Alarcon C, et al. Succinate Is a Preferential Metabolic Stimulus-Coupling Signal for Glucose-Induced Proinsulin Biosynthesis Translation. *Diabetes*. 2002;51(8):2496–2504.

18. Leibowitz G, et al. Mitochondrial regulation of insulin production in rat pancreatic islets. *Diabetologia*. 2005;48(8):1549–1559.

19. Huang M, Joseph JW. Assessment of the Metabolic Pathways Associated With Glucose-Stimulated Biphasic Insulin Secretion. *Endocrinology*. 2014;155(5):1653–1666.

20. Diehl J, et al. Expression and localization of GPR91 and GPR99 in murine organs. *Cell Tissue Res*. 2016;364(2):245–62.

21. Regard JB, Sato IT, Coughlin SR. Anatomical profiling of G protein-coupled receptor expression. *Cell*. 2008;135(3):561–71.

22. Amisten S, et al. An atlas and functional analysis of G-protein coupled receptors in human islets of Langerhans. *Pharmacol Ther*. 2013;139(3):359–391.

23. Ryan DG, et al. Coupling Krebs cycle metabolites to signalling in immunity and cancer. *Nat Metab*. 2019;1(1):16–33.

24. Keiran N, et al. SUCNR1 controls an anti-inflammatory program in macrophages to regulate the metabolic response to obesity. *Nat Immunol*. 2019;20(5):581–592.

25. McCreath KJ, et al. Targeted disruption of the SUCNR1 metabolic receptor leads to dichotomous effects on obesity. *Diabetes*. 2015;64(4):1154–67.

26. van Diepen JA, et al. SUCNR1-mediated chemotaxis of macrophages aggravates obesity-induced inflammation and diabetes. *Diabetologia*. 2017;60(7):1304–1313.

27. Atallah R, et al. SUCNR1 Is Expressed in Human Placenta and Mediates Angiogenesis: Significance in Gestational Diabetes. *Int J Mol Sci*. 2021;22(21).

28. Correa PRA V, et al. Succinate is a paracrine signal for liver damage. *J Hepatol*. 2007;47(2):262–9.

29. Mills EL, et al. UCP1 governs liver extracellular succinate and inflammatory pathogenesis. *Nat Metab*. 2021;3(5):604–617.

30. Le CT, et al. LY2405319, an analog of fibroblast growth factor 21 ameliorates α-smooth muscle actin production through inhibition of the succinate-G-protein couple receptor 91 (GPR91) pathway in mice. *PLoS One*. 2018;13(2):e0192146.

31. Nguyen G, et al. Metformin ameliorates activation of hepatic stellate cells and hepatic fibrosis by succinate and GPR91 inhibition. *Biochem Biophys Res Commun*. 2018;495(4):2649–2656.

32. Hochachka PW, Dressendorfer RH. Succinate accumulation in man during exercise. *Eur J Appl Physiol Occup Physiol*. 1976;35(4):235–42.

33. Astiarraga B, et al. Impaired Succinate Response to a Mixed Meal in Obesity and Type 2 Diabetes Is Normalized After Metabolic Surgery. *Diabetes Care*. 2020;43(10):2581–2587.

34. He W, et al. Citric acid cycle intermediates as ligands for orphan G-protein-coupled receptors. *Nature*. 2004;429(6988):188–193.

35. Högberg C, et al. Succinate independently stimulates full platelet activation via cAMP and phosphoinositide 3-kinase-β signaling. *J Thromb Haemost*. 2011;9(2):361–72.

36. Trauelsen M, et al. Extracellular succinate hyperpolarizes M2 macrophages through SUCNR1/GPR91-mediated Gq signaling. *Cell Rep*. 2021;35(11):109246.

37. Zawalich WS, Rasmussen H. Control of insulin secretion: a model involving Ca2+, cAMP and diacylglycerol. *Mol Cell Endocrinol*. 1990;70(2):119–137.

38. Guo Y, et al. Multifaceted Actions of Succinate as a Signaling Transmitter Vary with Its Cellular Locations. *Endocrinol Metab (Seoul)*. 2020;35(1):36.

39. Walker JT, et al. The Human Islet: Mini-Organ With Mega-Impact. *Endocr Rev*. 2021;42(5):605–657.

40. Mularoni L, Ramos-Rodríguez M, Pasquali L. The Pancreatic Islet Regulome Browser. *Front Genet*. 2017;8:13.

41. Servitja JM, Ferrer J. Transcriptional networks controlling pancreatic development and beta cell function. *Diabetologia*. 2004;47(4):597–613.

42. Pasquali L, et al. Pancreatic islet enhancer clusters enriched in type 2 diabetes risk-associated variants. *Nat Genet*. 2014;46(2):136–143.

43. Shrestha S, et al. Combinatorial transcription factor profiles predict mature and functional human islet α and β cells. *JCI Insight*. 2021;6(18).

44. Morán I, et al. Human β cell transcriptome analysis uncovers lncRNAs that are tissue-specific, dynamically regulated, and abnormally expressed in type 2 diabetes. *Cell Metab*. 2012;16(4):435–48.

45. Bonàs-Guarch S, et al. Re-analysis of public genetic data reveals a rare X-chromosomal variant associated with type 2 diabetes. *Nat Commun*. 2018;9(1):321.

46. Fahien LA, MacDonald MJ. The succinate mechanism of insulin release. *Diabetes*. 2002;51(9):2669–76.

47. Geubelle P, et al. Identification and pharmacological characterization of succinate receptor agonists. *Br J Pharmacol*. 2017;174(9):796–808.

48. Pajor AM. Sodium-coupled dicarboxylate and citrate transporters from the SLC13 family. *Pflugers Arch*. 2014;466(1):119–30.

49. Pajor AM. Molecular properties of the SLC13 family of dicarboxylate and sulfate transporters. *Pflugers Arch*. 2006;451(5):597–605.

50. Ryaboshapkina M, et al. Characterization of the Secretome, Transcriptome, and Proteome of Human β Cell Line EndoC-βH1. *Mol Cell Proteomics*. 2022;21(5):100229.

51. Blanchi B, et al. EndoC-βH5 cells are storable and ready-to-use human pancreatic beta cells with physiological insulin secretion. *Mol Metab*. 2023;76:101772.

52. Haffke M, et al. Structural basis of species-selective antagonist binding to the succinate receptor. *Nature*. 2019;574(7779):581–585.

53. Gilissen J, et al. Insight into SUCNR1 (GPR91) structure and function. *Pharmacol Ther*. 2016;159:56–65.

54. Antunes CM, et al. Differential patterns of glucose-induced electrical activity and intracellular calcium responses in single mouse and rat pancreatic islets. *Diabetes*. 2000;49(12):2028–2038.

55. Shigeto M, et al. GLP-1 stimulates insulin secretion by PKC-dependent TRPM4 and TRPM5 activation. *J Clin Invest*. 2015;125(12):4714–28.

56. Arkhammar P, et al. Protein kinase C modulates the insulin secretory process by maintaining a proper function of the beta-cell voltage-activated Ca2+ channels. *J Biol Chem*. 1994;269(4):2743–9.

57. Ahn D, Ham D, Chung KY. The conformational transition during G protein–coupled receptor (GPCR) and G protein interaction. *Curr Opin Struct Biol*. 2021;69:117–123.

58. Rozengurt E. Mitogenic signaling pathways induced by G protein-coupled receptors. *J Cell Physiol*. 2007;213(3):589–602.

59. Thorens B, et al. Ins1 Cre knock-in mice for beta cell-specific gene recombination. *Diabetologia*. 2015;58(3):558–565.

60. American Diabetes Association. Standards of Medical Care for Patients With Diabetes Mellitus. *Diabetes Care*. 2003;26(suppl_1):s33–s50.

61. Serena C, et al. Elevated circulating levels of succinate in human obesity are linked to specific gut microbiota. *ISME J*. 2018;12(7):1642–1657.

62. Ceperuelo-Mallafré V, et al. Preoperative Circulating Succinate Levels as a Biomarker for Diabetes Remission After Bariatric Surgery. *Diabetes Care*. 2019;42(10):1956–1965.

63. Thor D. G protein-coupled receptors as regulators of pancreatic islet functionality. *Biochim Biophys Acta Mol Cell Res*. 2022;1869(5):119235.

64. Seino S, et al. β-Cell signalling and insulin secretagogues: A path for improved diabetes therapy. *Diabetes Obes Metab*. 2017;19:22–29.

65. Zawalich WS, Zawalich KC. Species differences in the induction of time-dependent potentiation of insulin secretion. *Endocrinology*. 1996;137(5):1664–1669.

66. MacDonald MJ. Differences between mouse and rat pancreatic islets: succinate responsiveness, malic enzyme, and anaplerosis. *Am J Physiol Endocrinol Metab*. 2002;283(2):E302–E310.

67. Robben JH, et al. Localization of the succinate receptor in the distal nephron and its signaling in polarized MDCK cells. *Kidney Int*. 2009;76(12):1258–1267.

68. Gilissen J, et al. Forskolin-free cAMP assay for Gi-coupled receptors. *Biochem Pharmacol*. 2015;98(3):381–91.

69. Sundström L, et al. Succinate receptor GPR91, a Gα i coupled receptor that increases intracellular calcium concentrations through PLCβ. *FEBS Lett*. 2013;587(15):2399–2404.

70. Tang X, et al. Activation of succinate receptor 1 boosts human mast cell reactivity and allergic bronchoconstriction. *Allergy*. 2022;77(9):2677–2687.

71. Mancini AD, Poitout V. The fatty acid receptor FFA1/GPR40 a decade later: how much do we know? *Trends Endocrinol Metab*. 2013;24(8):398–407.

72. Itoh Y, et al. Free fatty acids regulate insulin secretion from pancreatic β cells through GPR40. *Nature 2003 422:6928*. 2003;422(6928):173–176.

73. Rajan S, et al. Chronic hyperglycemia downregulates GLP-1 receptor signaling in pancreatic β-cells via protein kinase A. *Mol Metab*. 2015;4(4):265–276.

74. Xu G, et al. Downregulation of GLP-1 and GIP Receptor Expression by Hyperglycemia. *Diabetes*. 2007;56(6):1551–1558.

75. Steinthorsdottir V, et al. Identification of low-frequency and rare sequence variants associated with elevated or reduced risk of type 2 diabetes. *Nat Genet*. 2014;46(3):294–8.

76. Macias-Ceja DC, et al. Succinate receptor mediates intestinal inflammation and fibrosis. *Mucosal Immunol*. 2019;12(1):178–187.

77. Mu X, et al. Oncometabolite succinate promotes angiogenesis by upregulating VEGF expression through GPR91-mediated STAT3 and ERK activation. *Oncotarget*. 2017;8(8):13174–13185.

78. Littlewood-Evans A, et al. GPR91 senses extracellular succinate released from inflammatory macrophages and exacerbates rheumatoid arthritis. *J Exp Med*. 2016;213(9):1655–62.

79. Aguiar CJ, et al. Succinate causes pathological cardiomyocyte hypertrophy through GPR91 activation. *Cell Commun Signal*. 2014;12:78.

80. Toma I, et al. Succinate receptor GPR91 provides a direct link between high glucose levels and renin release in murine and rabbit kidney. *J Clin Invest*. 2008;118(7):2526–34.

81. Sapieha P, et al. The succinate receptor GPR91 in neurons has a major role in retinal angiogenesis. *Nat Med*. 2008;14(10):1067–1076.

82. Osuna-Prieto FJ, et al. Elevated plasma succinate levels are linked to higher cardiovascular disease risk factors in young adults. *Cardiovasc Diabetol*. 2021;20(1).

83. Sadagopan N, et al. Circulating succinate is elevated in rodent models of hypertension and metabolic disease. *Am J Hypertens*. 2007;20(11):1209–15.

84. Villanueva-Carmona T, et al. SUCNR1 signaling in adipocytes controls energy metabolism by modulating circadian clock and leptin expression. *Cell Metab*. 2023;35(4):601-619.e10.

85. Saisho Y, et al. β-Cell mass and turnover in humans: Effects of obesity and aging. *Diabetes Care*. 2013;36(1):111–117.

86. Reaven GM, Hollenbeck CB, Chen Y-DI. Relationship between glucose tolerance, insulin secretion, and insulin action in non-obese individuals with varying degrees of glucose tolerance. *Diabetologia*. 1989;32(1).

87. Holst JJ. The incretin system in healthy humans: The role of GIP and GLP-1. *Metabolism*. 2019;96:46–55.

88. Hu J, et al. Inhibition of high glucose-induced VEGF release in retinal ganglion cells by RNA interference targeting G protein-coupled receptor 91. *Exp Eye Res*. 2013;109:31–9.

89. Brownlee M. The pathobiology of diabetic complications: a unifying mechanism. *Diabetes*. 2005;54(6):1615–25.

90. Pingitore A, et al. The diet-derived short chain fatty acid propionate improves beta-cell function in humans and stimulates insulin secretion from human islets in vitro. *Diabetes Obes Metab*. 2017;19(2):257–265.

91. Priyadarshini M, et al. An Acetate-Specific GPCR, FFAR2, Regulates Insulin Secretion. *Mol Endocrinol*. 2015;29(7):1055–1066.

92. Rubic T, et al. Triggering the succinate receptor GPR91 on dendritic cells enhances immunity. *Nat Immunol*. 2008;9(11):1261–9.

93. Huber-Ruano I, et al. Orally administered Odoribacter laneus improves glucose control and inflammatory profile in obese mice by depleting circulating succinate. *Microbiome*. 2022;10(1):135.

94. Mari A, et al. A Model-Based Method for Assessing Insulin Sensitivity From the Oral Glucose Tolerance Test. *Diabetes Care*. 2001;24(3):539–548.

95. Tura A, et al. Altered pattern of the incretin effect as assessed by modelling in individuals with glucose tolerance ranging from normal to diabetic. *Diabetologia*. 2014;57(6):1199–1203.

96. Van Cauter E, et al. Estimation of insulin secretion rates from C-peptide levels. Comparison of individual and standard kinetic parameters for C-peptide clearance. *Diabetes*. 1992;41(3):368–77.

97. Mari A, et al. Meal and oral glucose tests for assessment of β-cell function: modeling analysis in normal subjects. *Am J Physiol Endocrinol Metab*. 2002;283(6):E1159–E1166.

98. Alquier T, Poitout V. Considerations and guidelines for mouse metabolic phenotyping in diabetes research. *Diabetologia*. 2018;61(3):526–538.

99. Ravassard P, et al. A genetically engineered human pancreatic β cell line exhibiting glucose-inducible insulin secretion. *J Clin Invest*. 2011;121(9):3589–3597.

100. Scharfmann R, Staels W, Albagli O. The supply chain of human pancreatic β cell lines. *Journal of Clinical Investigation*. 2019;129(9):3511–3520.

101. De Jesus DF, et al. m6A mRNA methylation regulates human β-cell biology in physiological states and in type 2 diabetes. *Nat Metab*. *2019 1:8*. 2019;1(8):765–774.

102. Ishihara H, et al. Pancreatic beta cell line MIN6 exhibits characteristics of glucose metabolism and glucose-stimulated insulin secretion similar to those of normal islets. *Diabetologia*. 1993;36(11):1139–45.

TABLES

Table 1. Clinical and anthropometric data of the subjects included in the study

	Normal Glucose Tolerant	Non-Normal Glucose Tolerant	*p*
n (female/male)	12 (9/3)	18 (8/10)	
Age (years)	36.2 ± 12.7	45.6 ± 11.0	0.039
BMI ($kg \cdot m^{-2}$)	26.3 ± 2.8	30.5 ± 3.5	<0.001
Waist-to-hip (cm)	0.86 ± 0.07	0.94 ± 0.10	0.028
Fat mass (%)	31.5 ± 7.3	33.9 ± 6.8	0.373
FPG ($mg \cdot dl^{-1}$)	94.9 ± 4.8	106.0 ± 10.2	<0.001
Uric acid ($mg \cdot dl^{-1}$)	4.3 ± 1.0	5.8 ± 1.2	0.010
Total cholesterol ($mg \cdot dl^{-1}$)	155.8 ± 32.5	182.6 ± 36.4	0.049
HDL ($mg \cdot dl^{-1}$)	53.3 ± 10.1	51.7 ± 11.5	0.686
LDL ($mg \cdot dl^{-1}$)	86.5 ± 23.2	111.8 ± 32.0	0.026
Triglycerides ($mg \cdot dl^{-1}$)	80.4 ± 33.4	114.6 ± 64.6	0.084
AST ($U \cdot l^{-1}$)	17.8 ± 3.7	34.2 ± 22.4	0.002
ALT ($U \cdot l^{-1}$)	15.0 ± 4.3	27.2 ± 10.5	<0.001
GGT ($U \cdot l^{-1}$)	15.8 ± 7.0	58.9 ± 64.8	0.002
HbA1c (%)	5.1 ± 0.3	5.4 ± 0.3	0.005
2-h glucose ($mg \cdot dl^{-1}$)	120.4 ± 15.4	154.1 ± 40.5	0.003
Fasting insulin ($pmol \cdot l^{-1}$)	49.1 ± 14.6	64.9 ± 31.0	0.072
Fasting C-peptide ($nmol \cdot l^{-1}$)	0.33 ± 0.08	0.47 ± 0.19	0.030
Fasting GLP-1 ($pmol \cdot l^{-1}$)	24.0 ± 7.7	31.6 ± 17.7	0.121
Fasting succinate ($\mu mol \cdot l^{-1}$)	47.8 ± 22.6	60.8 ± 23.3	0.142
OGIS ($ml \cdot min^{-1} \cdot m^{-2}$)	406.6 ± 30.7	331.3 ± 51.0	<0.001
Incretin effect (a.u.)	1.78 ± 0.66	1.43 ± 0.36	0.114

Abbreviations: body mass index (BMI), fasting plasma glucose (FPG), high-density lipoprotein (HDL), low-density lipoprotein (LDL), aspartate aminotransferase (AST), alanine aminotransferase (ALT), gamma-glutaryl transferase (GGT), hemoglobin A1c (HbA1c), glucagon-like peptide 1 (GLP-1), oral glucose insulin sensitivity (OGIS), arbitrary units (a.u.). Data are presented as mean ± SD. *p*-value was determined by the Student's *t*-test (with Welch's correction if SD is inconsistent between groups) or the Mann-Whitney *U*-test according to the data distribution.

FIGURES

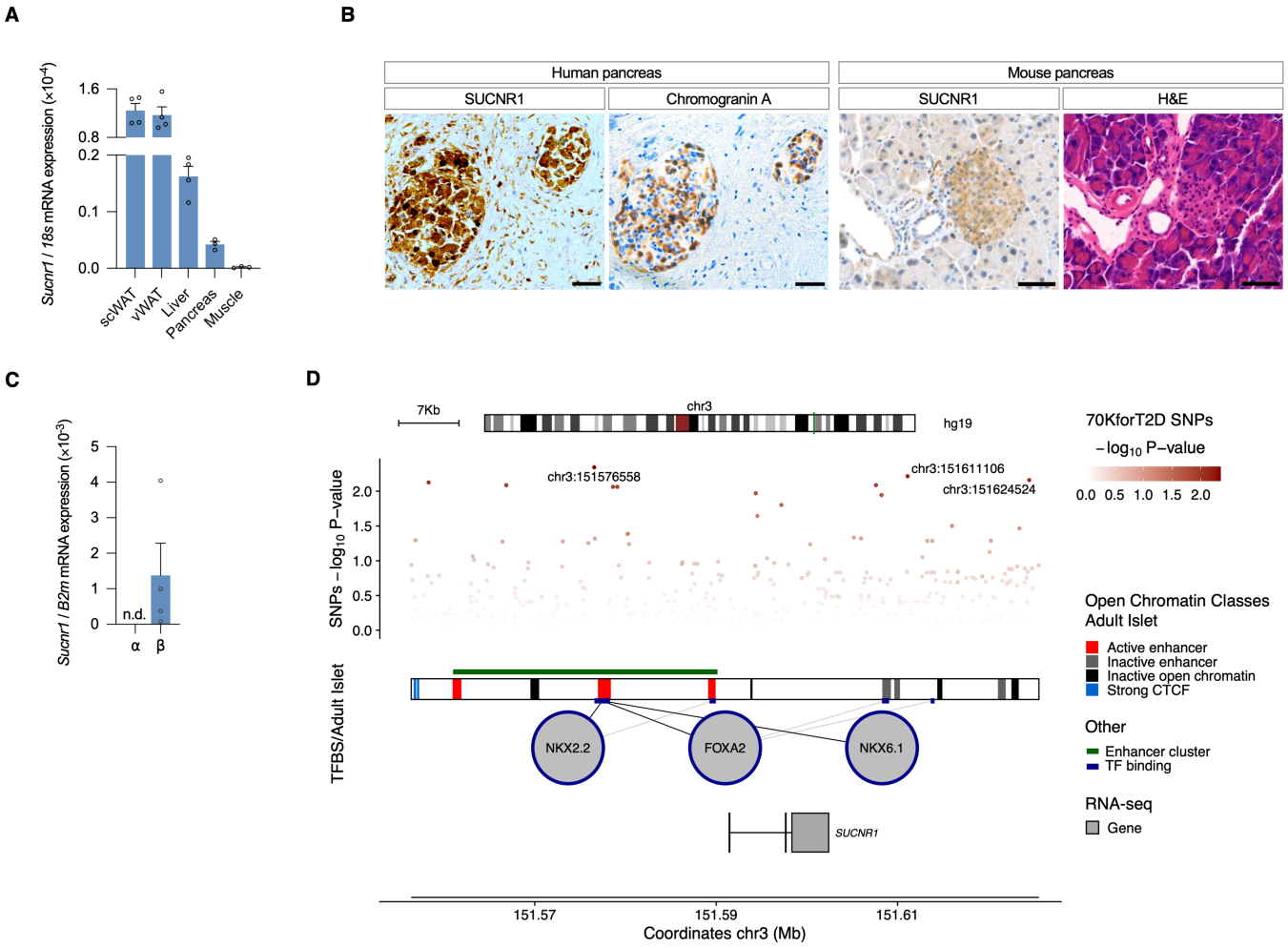

Figure 1: SUCNR1 is expressed in islets and β-cells. (**A)** *Sucnr1* mRNA levels analyzed in subcutaneous white adipose tissue (scWAT), visceral WAT (vWAT), liver, pancreas, and muscle tissue from male mice by qPCR (n=3-4). **(B)** Immunohistochemical (IHC) staining of SUCNR1 in male human and male mouse pancreas sections, and chromogranin A IHC staining or hematoxylin and eosin (H&E) staining. Scale bars represent 50 µm. **(C)** Analysis of *Sucnr1* mRNA expression in α- and β-cells isolated by fluorescence-activated cell sorting (FACS) from male rat islets (n=4). **(D)** *In silico* study of *SUCNR1* gene expression regulation by genomic sequences and specific human adult islet transcriptional factors, and single nucleotide polymorphisms (SNPs) associated with type 2 diabetes (T2D) localized within or surrounding the *SUCNR1* locus. Data are presented as mean ± SEM.

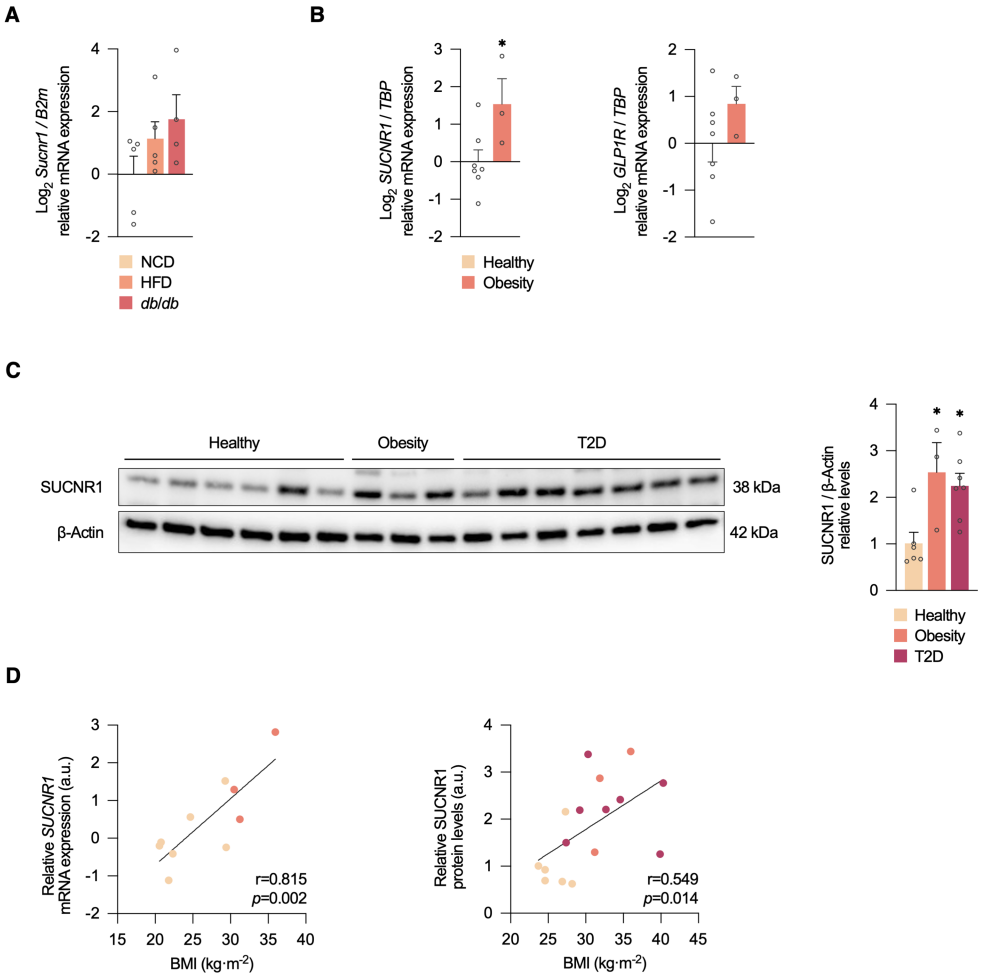

Figure 2: SUCNR1 levels in islets are dysregulated in obesity and type 2 diabetes. (A) *Sucnr1* mRNA expression in the entire pancreas of normal-chow diet (NCD)- and high-fat diet (HFD)-fed wild-type mice, and *db/db* mice on NCD (n=4-5). **(B)** *SUCNR1* and *GLP1R* mRNA expression in islets from healthy (n=7) and donors with obesity (n=3). **(C)** SUCNR1 protein levels in human islet lysates from healthy (n=6) and donors with obesity (n=3) and T2D (n=7). **(D)** Linear correlations between the body mass index (BMI) of donors and SUCNR1 mRNA (n=10) and protein (n=16) expression. Data are presented as mean ± SEM. *$p<0.05$ vs control (Student's *t*-test in **(A)** and **(B)**, Kruskal-Wallis test with Dunn's test for multiple comparisons in **(C)**, or Pearson's correlation coefficient in **(D)**).

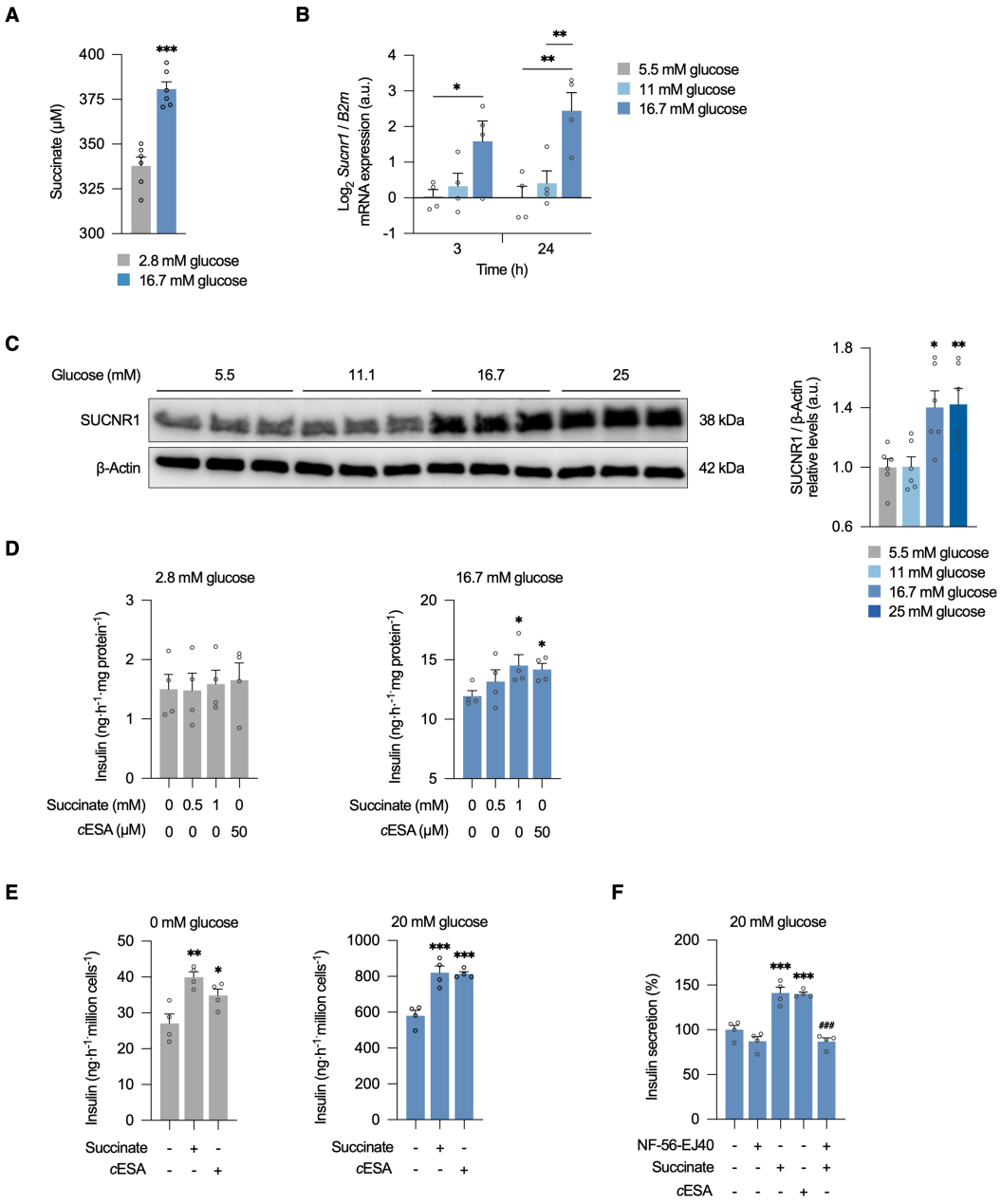

Figure 3: The Succinate/SUCNR1 axis enhances glucose-stimulated insulin secretion in β-cells. (A) Succinate quantification in the conditioned media (CM) of MIN6 cells cultured in low- or high-glucose conditions (n=6). **(B)** *Sucnr1* mRNA expression in MIN6 cells stimulated with different concentrations of glucose for 3 or 24 hours (n=4). **(C)** SUCNR1 protein levels in EndoC-βH1 cells stimulated with different concentrations of glucose for 24 hours (n=6). **(D)** Insulin quantification in the CM of MIN6 cells stimulated with succinate or *cis*-epoxysuccinic acid (*c*ESA) at 2.8 mM or 16.7 mM glucose (n=4). **(E)** Insulin secretion in glucose-stimulated insulin secretion assays in EndoC-βH5 cells stimulated with 500 µM succinate or 50 µM *c*ESA at 0 mM or 20 mM glucose, determined in the CM by ELISA (n=4). **(F)** Insulin secretion in EndoC-βH5 cells incubated with a human-specific SUCNR1 antagonist (1 µM NF-56-EJ40) and 500 µM succinate or 50 µM *c*ESA (n=4). Data are presented as mean ± SEM. **p*<0.05, ***p*<0.01, ****p*<0.001 vs basal conditions; $^{\#\#\#}$*p*<0.001 vs succinate (Student's *t*-test in **(A)**, ANOVA with Dunnett's test for multiple comparisons in **(B-E)**, or ANOVA with Tukey's test for multiple comparisons in **(F)**).

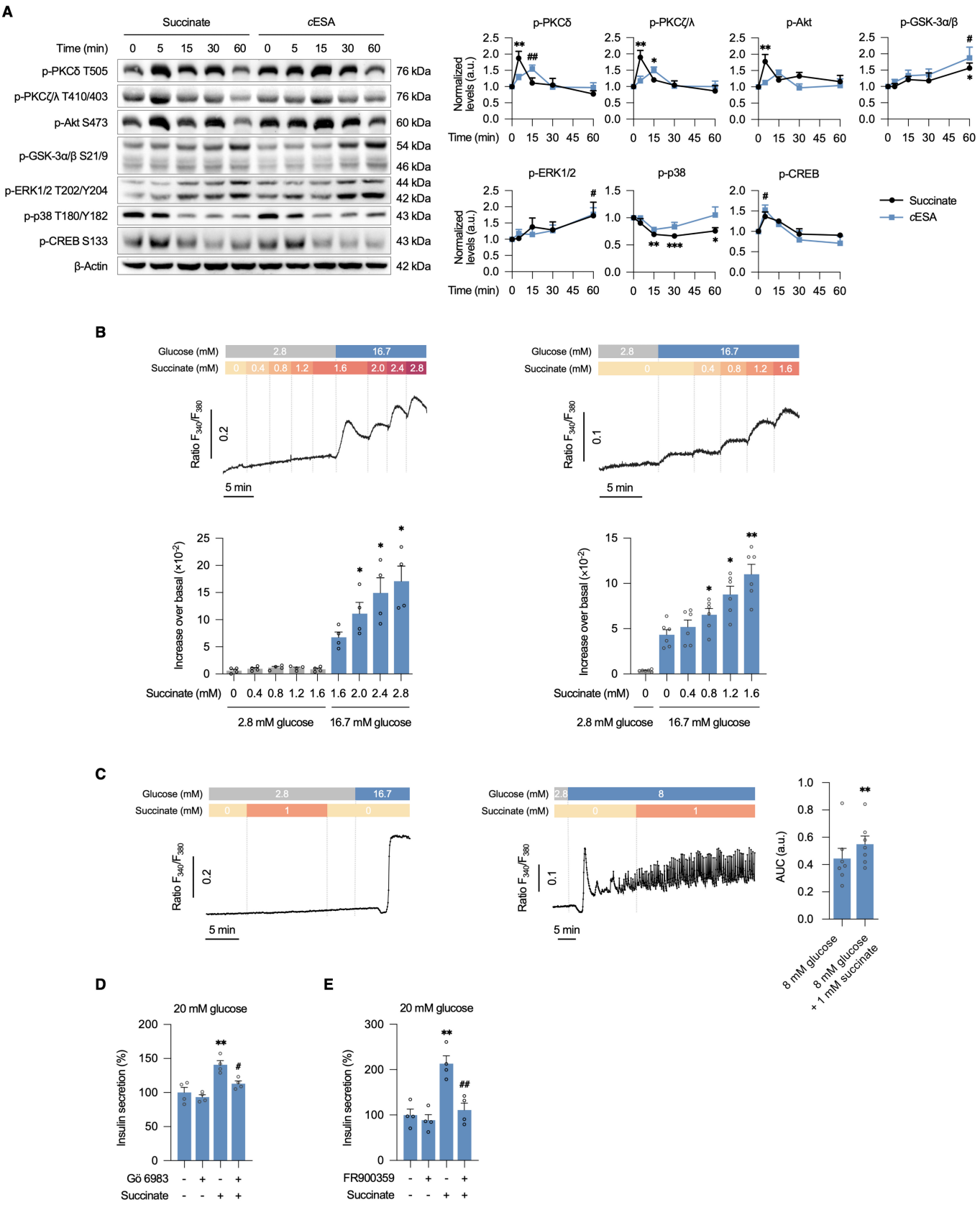
A
Succinate
cESA
Time (min)
p-PKCδ T505
p-PKCζ/λ T410/403
p-Akt S473
p-GSK-3α/β S21/9
p-ERK1/2 T202/Y204
p-p38 T180/Y182
p-CREB S133
β-Actin
76 kDa
60 kDa
54 kDa
46 kDa
44 kDa
42 kDa
43 kDa
Normalized levels (a.u.)
Succinate
cESA
B
Glucose (mM)
Succinate (mM)
Ratio F340/F380
5 min
Increase over basal (×10-2)
2.8 mM glucose
16.7 mM glucose
C
8 mM glucose
AUC (a.u.)
8 mM glucose + 1 mM succinate
D
20 mM glucose
Insulin secretion (%)
Gö 6983
Succinate
E
FR900359

Figure 4: SUCNR1 activation in β-cells induces proximal signaling and Ca^{2+} mobilization, and is dependent on Gq and PKC pathways in β-cells. (A) Western blot analysis of several phosphoproteins in MIN6 cells stimulated with 500 µM succinate or 50 µM *cis*-epoxysuccinic acid (*c*ESA) at different time points (n=4-5). **(B)** Ca^{2+} mobilization in MIN6 cells stimulated with glucose and succinate assessed by the Fura-2-AM fluorometric ratio. Left panel: a representative trace and quantification of the response to sequential increases in succinate concentration before and after high glucose exposure (n=4). Right panel: a representative trace and quantification of the response to succinate concentrations elevated similarly post high glucose exposure (n=6). **(C)** Intracellular Ca^{2+} mobilization in perifused islets from wild-type C57BL/6 male mice assessed by the Fura-2-AM fluorometric ratio. Left panel: a representative trace of 1 mM succinate's effect on intracellular Ca^{2+} mobilization at a basal glucose concentration (2.8 mM), followed by exposure to 16.7 mM glucose (n=7 islets from three mice). Right panel: a representative trace and quantification of 1 mM succinate effect on intracellular Ca^{2+} mobilization at 8 mM glucose (n=7 islets from two mice). **(D)** Insulin secretion in EndoC-βH5 cells incubated with 500 µM succinate and 1µM of the PKC inhibitor Gö 6983 (n=4). **(E)** Insulin secretion in EndoC-βH5 cells incubated with 500 µM succinate and the 1 µM of Gq inhibitor FR900359 (n=4). Data are presented as mean ± SEM. $^{*}p<0.05$, $^{**}p<0.01$, $^{***}p<0.001$ when comparing succinate with the basal condition; $^{\#}p<0.05$, $^{\#\#}p<0.01$, when comparing *c*ESA with the basal condition, or an inhibitor with succinate (ANOVA with Dunnett's test for multiple comparisons in **(A)** and **(B)**, paired Student's *t*-test in **(C)**, or ANOVA with Tukey's test for multiple comparisons in **(D)** and **(E)**).

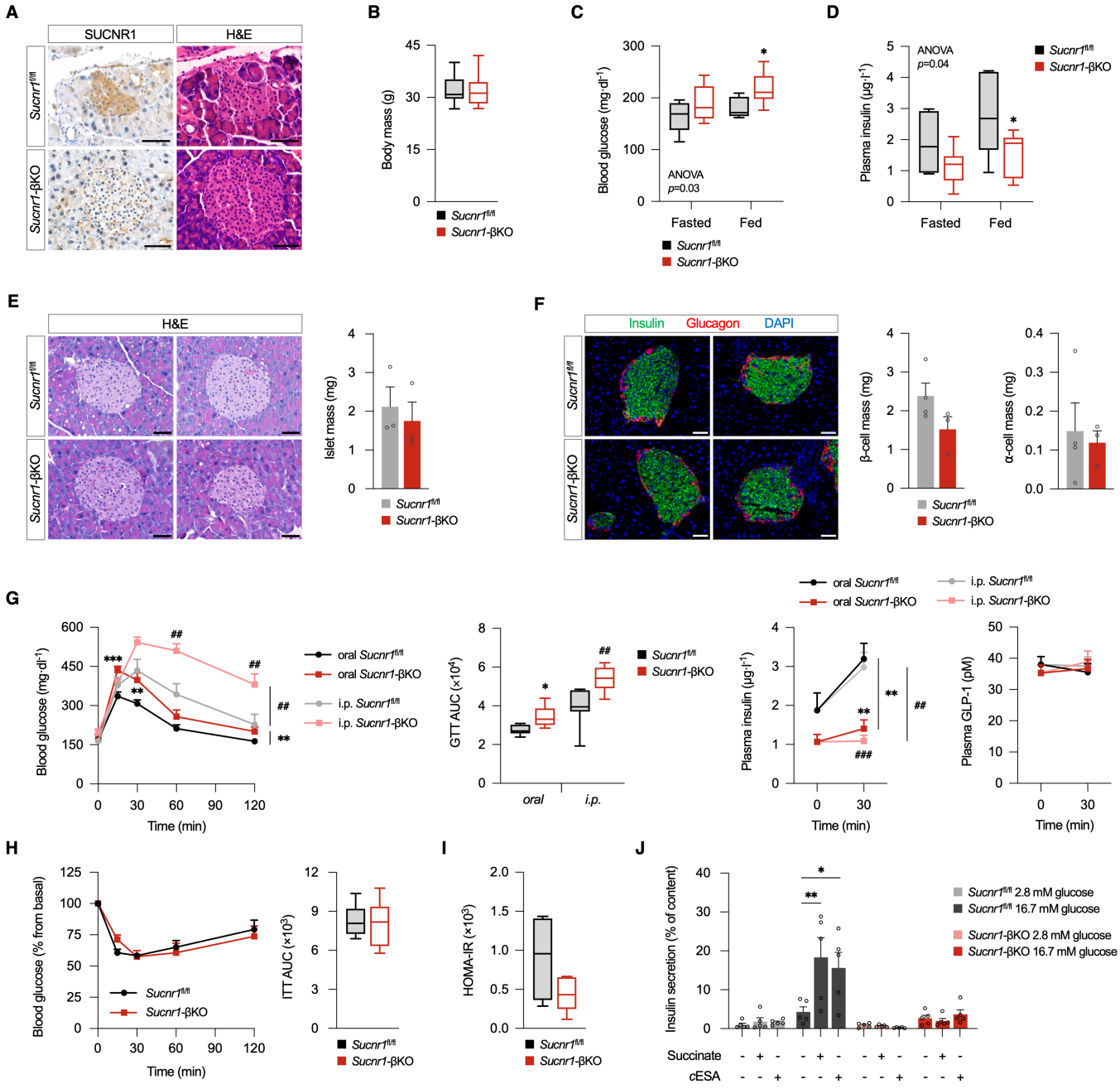

Figure 5: SUCNR1 in β-cells is required for preserving insulin secretion and glucose homeostasis in high-fat diet-fed male mice. (A) Immunohistochemical staining of SUCNR1 in pancreas sections of control and *Sucnr1*-βKO mice accompanied with serial hematoxylin and eosin (H&E) staining. Scale bar represents 50 µm. **(B)** Body mass of control and *Sucnr1*-βKO mice under HFD for 8 weeks (n=8-9). **(C)** Blood glucose levels in control and *Sucnr1*-βKO mice in fasted or random-fed conditions (n=8). **(D)** Plasma insulin levels in control and *Sucnr1*-βKO in fasted or random-fed conditions (n=7-8). **(E)** Morphometric analysis of control and *Sucnr1*-βKO mice by H&E staining (n=3). Scale bar indicates 50 µm. **(F)** Morphometric analysis of control and *Sucnr1*-βKO mice by immunofluorescence staining with insulin and glucagon and counterstained with DAPI (n=3-4). Scale bar indicates 50 µm. **(G)** Intraperitoneal (i.p.) and oral glucose tolerance tests in control and *Sucnr1*-βKO mice (n=6-7). Displayed are the blood glucose levels, area under the curve (AUC), plasma insulin (n=5-6), and GLP-1 levels (n=5). **(H)** Insulin tolerance test in control and *Sucnr1*-βKO mice (n=6-8). **(I)** HOMA-IR index for control and *Sucnr1*-βKO mice (n=5). **(J)** Insulin secretion in isolated islets from control and *Sucnr1*-βKO mice stimulated with or without 1 mM succinate or 100 µM *c*ESA at 2.8 or 16.7 mM glucose (n=5 islet pools from 5-6 mice). Data are presented as mean ± SEM or as box-and-whiskers plots indicating the median, first and third quartiles, and maximum and minimum values. *p<0.05, **p<0.01, ***p<0.001 vs control mice, when comparing experimental groups in orally-administered mice, or in indicated pair-wise comparisons; $^{\#\#}p$<0.01, $^{\#\#\#}p$<0.001 when comparing experimental groups in i.p.-administered mice (Student's *t*-test in **(B)**, **(E-F)** and **(I)** when comparing two groups or two-way ANOVA with Bonferroni's test for multiple comparisons in **(C-D)**, **(G-H)**, and **(J)**).

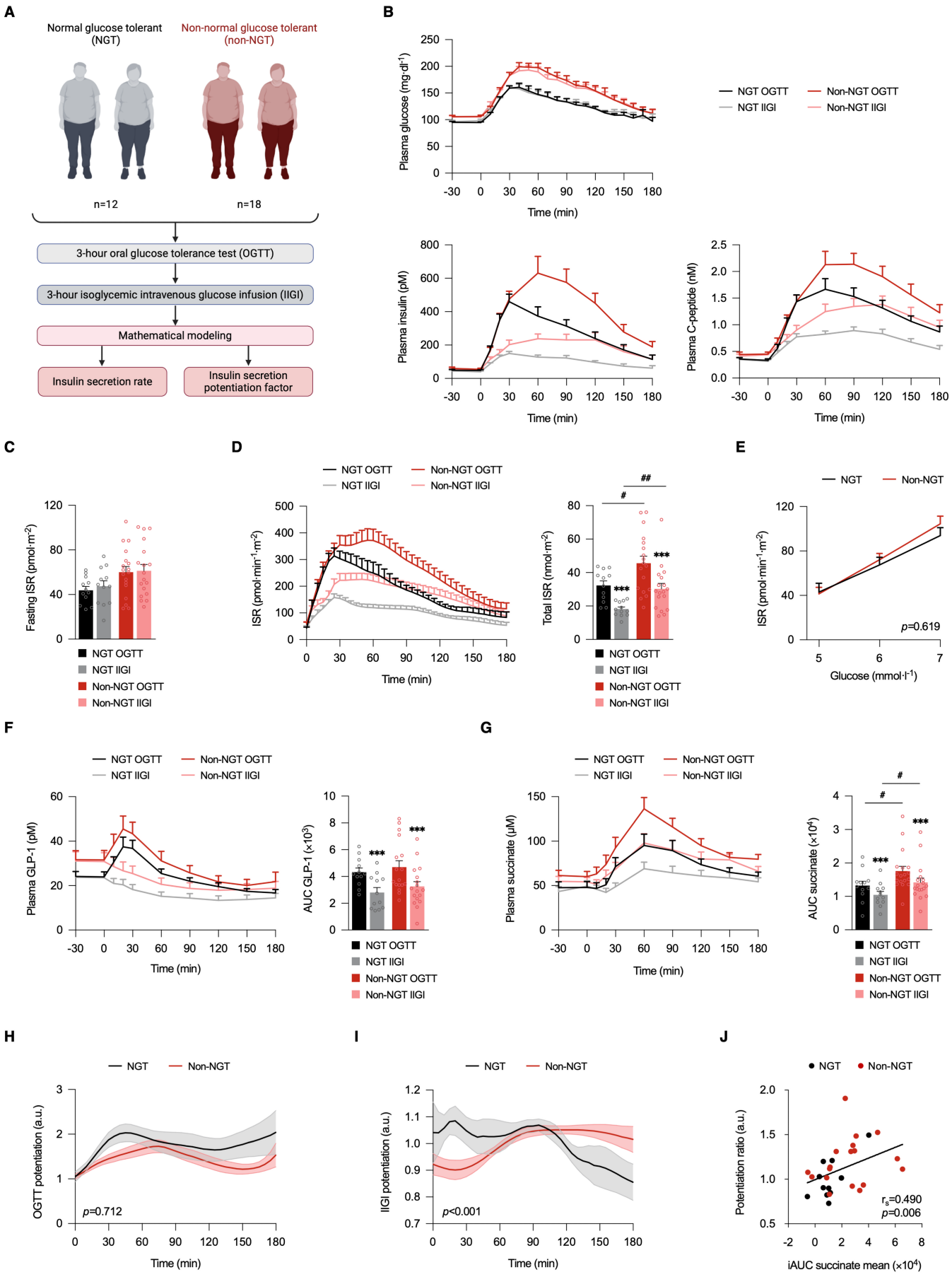
A
Normal glucose tolerant (NGT)
Non-normal glucose tolerant (non-NGT)
n=12
n=18
3-hour oral glucose tolerance test (OGTT)
3-hour isoglycemic intravenous glucose infusion (IIGI)
Mathematical modeling
Insulin secretion rate
Insulin secretion potentiation factor
B
Plasma glucose (mg·dl⁻¹)
Plasma insulin (pM)
Plasma C-peptide (nM)
Time (min)
NGT OGTT
NGT IIGI
Non-NGT OGTT
Non-NGT IIGI
C
Fasting ISR (pmol·m⁻²)
D
ISR (pmol·min⁻¹·m⁻²)
Total ISR (nmol·m⁻²)
E
NGT
Non-NGT
Glucose (mmol·l⁻¹)
p=0.619
F
Plasma GLP-1 (pM)
AUC GLP-1 (×10³)
G
Plasma succinate (μM)
AUC succinate (×10⁴)
H
OGTT potentiation (a.u.)
p=0.712
I
IIGI potentiation (a.u.)
p<0.001
J
Potentiation ratio (a.u.)
iAUC succinate mean (×10⁴)
r_s=0.490
p=0.006

Figure 6: Succinate response is heightened in non-normal glucose tolerant patients and is associated with the potentiation of insulin secretion. (A) Study cohort and study schematic. **(B)** Plasma glucose, insulin, and C-peptide levels during the oral glucose tolerance test (OGTT) and isoglycemic intravenous glucose infusion (IIGI) in normal glucose tolerant (NGT) (n=12) and non-normal glucose tolerant (non-NGT) (n=18) patients. **(C)** Fasting insulin secretion rate (ISR) in NGT and non-NGT groups. **(D)** ISR during OGTT and IIGI tests in NGT and non-NGT groups. **(E)** β-cell glucose sensitivity represented as a dose-response function between ISR and glucose concentrations for both groups. **(F)** Plasma GLP-1 levels during OGTT and IIGI for both groups. **(G)** Plasma succinate levels during OGTT and IIGI for both groups. **(H)** Incretin-related potentiation calculated during OGTT in relation to IIGI for both groups. **(I)** Potentiation calculated during IIGI for both groups. **(J)** Correlation between the potentiation factor mean and the area under the curve (AUC) of succinate during the IIGI for both groups (n=30). Data are presented as mean ± SEM. $^{***}p<0.001$ when comparing OGTT and IIGI; $^{\#}p<0.05$, $^{\#\#}p<0.01$, when comparing NGT and non-NGT subjects (paired and unpaired Student's *t*-tests in **(C), (D), (F),** and **(G)**; Mann-Whitney *U*-test in **(D), (F),** and **(G)**; Wilcoxon test in **(D) (F)** and **(G)**; two-way ANOVA tests in **(E-I)**; or Spearman's rank correlation coefficient in **(J)**).